

# BAERLIN2014 – stationary measurements and source apportionment at an urban background station in Berlin, Germany

Erika von Schneidmesser<sup>1</sup>, Boris Bonn<sup>1\*</sup>, Tim M. Butler<sup>1</sup>, Christian Ehlers<sup>2<sup>a</sup></sup>, Holger Gerwig<sup>3</sup>, Hannele Hakola<sup>4</sup>, Heidi Hellén<sup>4</sup>, Andreas Kerschbaumer<sup>5</sup>, Dieter Klemp<sup>2</sup>, Claudia Kofahl<sup>2<sup>b</sup></sup>, Jürgen Kura<sup>3</sup>, Anja Lüdecke<sup>3</sup>, Rainer Nothard<sup>5</sup>, Axel Pietsch<sup>3</sup>, Jörn Quedenau<sup>1</sup>, Klaus Schäfer<sup>6</sup>, James J. Schauer<sup>7</sup>, Ashish Singh<sup>1</sup>, Ana-Maria Villalobos<sup>7</sup>, Matthias Wiegner<sup>8</sup>, Mark G. Lawrence<sup>1</sup>

<sup>1</sup>Institute for Advanced Sustainability Studies (IASS), D-14467 Potsdam, Germany

<sup>2</sup>IEK-8, Research Centre Jülich, D-52425 Jülich, Germany

<sup>3</sup>Division Environmental Health and Protection of Ecosystems, German Environment Agency, D-06844 Dessau-Roßlau, Germany

<sup>4</sup>Finnish Meteorological Institute, FI-00560 Helsinki, Finland

<sup>5</sup>Senate Department for the Environment, Transport and Climate Protection, D-10179 Berlin, Germany

<sup>6</sup>Institute of Meteorology and Climate Research, Atmospheric Environmental Research (IMK-IFU), Karlsruhe Institute of Technology (KIT), D-82467 Garmisch-Partenkirchen, Germany

<sup>7</sup>Environmental Chemistry and Technology Program, University of Wisconsin-Madison, Madison 53705, WI, USA

<sup>8</sup>Ludwig-Maximilians-Universität, Meteorological Institute, D-80333 Munich, Germany

\*now at: Chair of Ecosystem Physiology, Institute of Forest Sciences, Albert-Ludwig Universität, D-79110 Freiburg, Germany

<sup>a</sup>now at: Fachbereich 42: Kontinuierliches Luftqualitätsmessnetz, Landesamt für Natur, Umwelt und Verbraucherschutz NRW, D-45133 Essen, Germany

<sup>b</sup>now at: Institut für Physikalische Chemie, Georg-August-Universität, D-37077 Göttingen, Germany

Correspondence to Erika von Schneidmesser ([evs@iass-potsdam.de](mailto:evs@iass-potsdam.de))

**Abstract.** The Berlin Air quality and Ecosystem Research: Local and long-range Impact of anthropogenic and Natural hydrocarbons (BAERLIN2014) campaign was conducted during the three summer months (June-August) of 2014. During this measurement campaign, both stationary and mobile measurements were undertaken to address complementary aims. This paper provides an overview of the stationary measurements and results that were focused on characterization of gaseous and particulate pollution, including source attribution, in the Berlin-Potsdam area, and quantification of the role of natural sources in determining levels of ozone and related gaseous pollutants. Results show that biogenic contributions to ozone and particulate matter are substantial. One indicator for ozone formation, the OH reactivity, showed a 31% ( $0.82 \pm 0.44 \text{ s}^{-1}$ ) and 75% ( $3.7 \pm 0.90 \text{ s}^{-1}$ ) contribution from biogenic NMVOCs for urban background ( $2.6 \pm 0.68 \text{ s}^{-1}$ ) and urban park ( $4.9 \pm 1.0 \text{ s}^{-1}$ ) location, respectively, emphasizing the importance of such locations as sources of biogenic NMVOCs in urban areas. A comparison to NMVOC measurements made in Berlin approx. 20 years earlier generally show lower levels today for anthropogenic NMVOCs. A substantial contribution of secondary organic and inorganic aerosol to PM<sub>10</sub> concentrations was quantified. In addition to secondary aerosols, source apportionment analysis of the organic carbon fraction identified the contribution of biogenic (plant-based) particulate matter, as well as primary contributions from vehicles, with a larger contribution from diesel compared to gasoline vehicles, as well as a relatively small contribution from wood burning, linked to measured levoglucosan.

## 45 1 Introduction

46

47 Air pollution and climate change are two of the most prescient environmental problems of our age. Recent  
48 research from the Global Burden of Disease study and others attribute over 3 million premature deaths to  
49 outdoor air pollution globally in 2013 (Brauer et al., 2016;Lelieveld et al., 2015;WHO, 2016). A report by the  
50 World Bank (WorldBank, 2016) estimated the 2013 welfare losses owing to ambient surface level PM<sub>2.5</sub> and O<sub>3</sub>  
51 air pollution to be equivalent to 5% of GDP in Europe, and often more in other world regions. Studies have  
52 shown that a changing climate will exacerbate ozone owing to increased temperatures and other factors, such as  
53 additional meteorological parameters and less effective emissions controls, that are favorable to ozone formation  
54 (Jacob and Winner, 2009;Rasmussen et al., 2013). One such factor is a projected increase in biogenic volatile  
55 organic compound emissions, such as isoprene or monoterpenes. While these increases are expected to be  
56 compensated for by much larger declines in anthropogenic emissions, as also indicated in other studies e.g.  
57 Colette et al. (2013) or West et al. (2013), there are additional impacts that are not yet captured by the models,  
58 such as those of secondary organic aerosol (SOA) among others, that show that such estimates of climate change  
59 effects are likely underestimated (Geels et al., 2015). While significant reductions in O<sub>3</sub> precursor emissions  
60 have been observed over the past couple decades, and peak ozone levels have been declining over much of  
61 north-western Europe, a comparable reduction in mean ozone has not followed (Derwent, 2008;Ehlers et al.,  
62 2016). This is particularly relevant for countries where the majority of the population resides in cities. In Europe  
63 during 2012-2014, more than 85% of the urban population has been exposed to air pollutant concentrations of  
64 ozone and PM<sub>2.5</sub> exceeding the recommended WHO limit values for the protection of human health, as well as  
65 substantial exceedances at the roadside of nitrogen dioxide (NO<sub>2</sub>) (EEA, 2016). In this context, it is crucial that  
66 we further improve our understanding of the sources of air pollutants in urban areas, as well as the contribution  
67 of natural sources to secondary pollutants such as ozone. Furthermore, recent research has shown that chemical  
68 products are emerging as the largest sources of non-methane volatile organic compounds in urban areas, owing  
69 to the previous regulatory focus on transport emissions (McDonald et al., 2018). An improved understanding of  
70 sources will allow for approaches that can better target the most relevant sources for mitigation, as well as  
71 accounting for the linkages between air quality and climate change in developing strategies for action on climate  
72 change and the reduction of air pollution, to improve health and create more livable cities.

73 The Berlin Air quality and Ecosystem Research: Local and long-range Impact of anthropogenic and  
74 Natural hydrocarbons 2014 (BAERLIN2014) campaign aimed to address some of these issues in the context of  
75 the Berlin-Potsdam urban area. The campaign had three main aims, (1) characterization of gaseous and  
76 particulate pollution, including source attribution, in the Berlin-Potsdam area, (2) quantification of the role of  
77 natural sources, specifically vegetation, in determining levels of gaseous pollutants, specifically ozone, and (3)  
78 improved understanding of the heterogeneity of pollutants throughout the city. In this paper, only aims (1) and  
79 (2) will be addressed. An overview paper describing the mobile measurements, which focused more on aim (3)  
80 was published previously (see Bonn et al. (2016)). Because of the focus on ozone and secondary pollutant  
81 formation, the campaign was conducted during the three summer months (June-August) of 2014, i.e. the time of  
82 maximum ozone pollution levels. Furthermore, while the mobile measurements covered the larger Berlin-  
83 Potsdam area, the stationary measurements were focused on an urban background location within the center of  
84 Berlin.

85           The unique characteristics of Berlin were particularly relevant to this study, in that it is a large urban  
86 area (population approx. 3.5 million) with significant vegetation. Of the approx. 890 km<sup>2</sup> that Berlin covers,  
87 approx. 34% of the land surface area is covered by vegetated areas and 6% by water (Senatsverwaltung für  
88 Stadtentwicklung III F, 2010). An existing air quality monitoring network (in German: Berliner Luftgüte  
89 Messnetz, abbreviated BLUME) provided data on which the campaign could build and leverage. Data from the  
90 16 stations that comprised the BLUME network showed that the EU 8-hour ozone target value of 120 µg m<sup>-3</sup> was  
91 exceeded 12-13 times at each of the two urban background stations that measure ozone (MC010 & MC042) and  
92 between 12-21 times per station at the stations on the periphery of the city (referred to here as Berlin rural  
93 stations) in 2014 (Stülpnagel et al., 2015). Six of these exceedances in the urban background occurred during the  
94 BAERLIN2014 campaign. Furthermore, the regulatory limit value for annual NO<sub>2</sub> of 40 µg m<sup>-3</sup> was exceeded at  
95 all six roadside stations in 2014, and although the annual PM<sub>10</sub> limit value was met, four out of five traffic  
96 stations where PM<sub>10</sub> was measured also exceeded the daily limit value of 50 µg m<sup>-3</sup> more than the allowed 35  
97 times; the exceedances at the urban background and Berlin rural stations ranged from 14 to 34 times (Stülpnagel  
98 et al., 2015). In short, the issue of air pollution has been recognized in Berlin as being in need of action. In this  
99 paper, we focus on the stationary measurements conducted at the urban background site in the Berlin city center.  
100 A brief overview is given of the suite of measurements conducted and the results obtained. This is followed by  
101 more detailed analysis of (1) the NMVOC data and the role in ozone formation including a comparison to a  
102 previous study in London and Paris (von Schneidemesser et al., 2011), as well as other urban areas, and (2)  
103 source apportionment analysis of PM<sub>10</sub> filter samples, including a rough comparison of the results to existing  
104 emission inventories.

105

## 106 **2 Methods**

107

108 A complete list of the parameters measured and their associated instrument descriptions are summarized in Table  
109 1.

110

### 111 **2.1 Site description**

112           The monitoring station that was the basis for the stationary measurements during the BAERLIN2014  
113 campaign was AirBase station DEBE034, which is maintained as part of the Berlin air quality measurement  
114 network (BLUME; BLUME network code MC042), and was located at the corner of Nansenstrasse and  
115 Framstrasse in the Neukölln district, in southeast central Berlin (52° 29' 21,98" N, 13° 25' 51,08" E) in a  
116 predominantly residential neighborhood, as shown in Figure 1. The station was located on the street corner next  
117 to a kindergarten and was classified as an urban background station. According to the location placement  
118 dictated by the EU Directive definition (EC, 2008), locations that are situated away from any strong point  
119 sources including major roads, typically in a residential neighborhood, but still in the urban core influenced by  
120 all sources upwind of the station are classified as urban background. These sites should in theory be  
121 representative of the general levels of pollution observed in a city and are used to assess exposure of the general  
122 population to air pollutants. This station will likely experience a comparatively high fraction of traffic-related  
123 emissions, since some fairly large inner-city thoroughfares were located within a 1 km radius of the site, but as  
124 appropriate for an urban background station will not be dominated by traffic like a site located at a major  
125 intersection. In addition, a measurement van was used to augment the capacity of the measurement station and

126 was located approximately 5 meters from the station, parked at the curb of the street (see Figure 1). Finally,  
127 owing to the presence of taller trees in that part of city, including in the vicinity of the monitoring station, one  
128 instrument (ceilometer) was located on the roof of the kindergarten to achieve an unobstructed view skywards,  
129 approximately 5 meters on the opposite side of the measurement station to the van.

130 A number of NMVOC canister samples were taken in locations throughout the city as part of the mobile  
131 measurements that augmented the stationary measurements in Neukölln. A subset of these were included in the  
132 companion paper to this one covering the mobile measurements (Bonn et al., 2016). These sites where multiple  
133 NMVOC canister samples were taken include Altlandsberg, Plänterwald, the Tiergarten Tunnel, and the so-  
134 called 'AVUS Motorway' during a traffic jam. Further details to the sampling environment can be found in  
135 Table 2. For more information on locations and/or sampling, see also Bonn et al. (2016).

136

## 137 **2.2 Instrument descriptions**

138 Complementing the BLUME measurements (see (Stülpnagel et al., 2015) or (Geiß et al., 2017) for  
139 details) were additional PM<sub>10</sub> filter samples collected for elemental carbon (EC) and organic carbon (OC), ions,  
140 and organic tracer analysis; intermittent canister and cartridge samples for the quantification of non-methane  
141 volatile organic compounds (NMVOCs) from an inlet next to the PM<sub>10</sub> inlet on the roof of the measurement  
142 station; a quadrupole Proton Transfer Reaction Mass Spectrometer (high sensitivity PTR-MS, Ionicon) up in the  
143 van for the measurement of NMVOCs; a set of particle instruments to measure number concentration, size  
144 distribution and surface area also located in the van (section 2.2.4); and a ceilometer CL51 (Vaisala GmbH,  
145 Hamburg) situated on the roof of the kindergarten. A complete list of instruments, parameters measured, and  
146 references for the methods used are provided in Table 1. Further details for the NMVOC measurements are  
147 provided in Table S1. Additional information is provided below.

148

### 149 **2.2.1 NMVOC Canister Samples**

150 The canisters were prepared to remove ozone using a heated silco-steel capillary (120 °C) prior to  
151 sampling. The cylinders were then pressurized using synthetic air to reduce the relative humidity of the sample.  
152 All NMVOC canister samples taken at Neukölln had a 20 minute sampling duration. After sampling, the  
153 canisters were promptly shipped to FZJ for analysis by GC-FID-MS and were analyzed with no more than five  
154 days between sampling and analysis. Analysis was done using a gas chromatographic system based on a  
155 conventional gas chromatograph (Agilent 6890) equipped with a flame ionization detector (FID), and a mass  
156 spectrometer (Agilent 5975C MSD) for the identification of the trace species. To analyze VOCs at trace gas  
157 levels, a cryogenic pre-concentration was used, consisting of a sample loop (silco steel, 20 cm length, inner  
158 diameter 2 mm) which was cooled down with cold gas above liquid nitrogen (see also Figure 14 in Ehlers et al.,  
159 (2016)). A volume of 800 mL was pre-concentrated in the sample loop at a flow of 80 mL min<sup>-1</sup>.

160 Subsequently, the sample was thermally desorbed at 120° C and injected on a capillary column (DB-1,  
161 120 m, 0.32 mm ID, 3µm film thickness). After injection, the column was kept isothermal at -60°C for 5 min,  
162 then heated to 200° C at a rate of 4° min<sup>-1</sup> and finally maintained at 220° C for 10 min. Signals were gathered  
163 from a flame ionization detector and a MSD, which each received 50% of the column output through a split  
164 valve. Analysis of one sample lasted for about 90 min, and sets of 10 cylinders (stainless steel canister, volume:  
165 6 L, Supelco Co., Bellefonte, PA, USA) could be analyzed by unattended operation.

166 The impact of canister transport and storage was assessed: C<sub>2</sub> - C<sub>11</sub> alkanes, alkenes and aromatic  
167 compounds were found to be stable within 5% over three days compared with an instantaneously analysed  
168 sample. Oxygenated compounds differed by up to 10% and terpenes by up to 20% over the same time period  
169 (Hengst, 2007). In addition, measurement accuracy depends on the uncertainty of the calibration standard (< 5%  
170 between true and declared gas concentrations, Apel-Riemer Environmental Inc.) and that of the mass-flow  
171 controller (< 2% deviation, MKS Instruments, Wilmington, MA, USA). Integration uncertainties ( $\Delta\mu\text{VOC}$ ) of  
172 the peak areas were dependent on their respective detection limits (DL<sub>i</sub>), which are estimated as in equation 1.

$$173 \quad \Delta\mu\text{VOC}_i \approx \begin{cases} DL_i & \text{for } \mu\text{VOC}_i \text{ next to } DL_i \\ (0,03-0,06)*\mu\text{VOC}_i & \text{otherwise} \end{cases} \quad (1)$$

174 Apart from concentrations and their respective detection limits geometrical addition of all these factors yielded  
175 overall experimental uncertainties of less than 10% (for a detailed discussion refer to Urban (2010)).  
176

### 177 2.2.1.1 Canister Samples and OH Reactivity Calculations

178 While a total of 103 compounds were quantified by GC-MS in the canister samples, not all of those  
179 compounds were regularly detected in the samples. Furthermore, to be able to make reasonable comparisons  
180 with previous work regarding the contribution of different compound classes to the measured mixing ratios of  
181 NMVOCs, as well as the OH reactivity attributed to these NMVOCs, a subset of the compounds was selected  
182 and used in the analysis. This subset was based on a number of papers in the literature that were also done in  
183 urban areas, and those compounds that were regularly included in OH reactivity calculations (e.g. (Dolgorouky  
184 et al., 2012; Gilman et al., 2009; Goldan et al., 2004; Liu et al., 2008)). This includes 57 NMVOCs (see SI).  
185 Furthermore, even if all compounds were included, there would still be missing reactivity that is not captured  
186 and because no OH measurements were made, the amount of missing reactivity cannot be reliably quantified,  
187 therefore the measured OH reactivity here is a lower limit. Owing to an undetermined source of contamination at  
188 the urban background site, the measurement of n-butane was compromised, and was therefore not included  
189 among the NMVOCs despite typically being reported in the literature. The data subsequently presented in this  
190 paper from the canister samples includes only these 57 compounds unless otherwise noted. For a complete list of  
191 the 103 compounds measured in the samples, including the concentrations reported for a subset of the samples  
192 discussed here, please see Bonn et al. (2016).

193 A number of canister samples were taken at different locations throughout the city, some with multiple  
194 measurements and some single samples. Five locations had multiple samples, including the main measurement  
195 site at the urban background station (DEBE034) in Neukölln (n=18), Plänterwald (n=11), Altlandsberg (n=10),  
196 the Tiergarten Tunnel (n=9), and the AVUS motorway during a traffic jam (n=2). All samples were taken during  
197 the month of August, will all samples except those in Neukölln taken on one day for any given location (Bonn et  
198 al., 2016). The samples in the Tiergarten tunnel and on the motorway are most indicative of NMVOC emissions  
199 from traffic.

### 201 2.2.2 NMVOC Cartridge Samples

202 NMVOCs (aromatic hydrocabons, terpenes, C<sub>6</sub>-C<sub>10</sub> alkanes) were collected into stainless steel  
203 cartridges (6.3 mm ED x 90 mm, 5.5 mm ID) filled with Tenax-TA (60/80 mesh, Supelco, Bellafonte, USA) and

204 CarboBack-B (60/80 mesh, Supelco, Bellefonte, USA) by using a flow rate of 100 ml min<sup>-1</sup> with a sampling time  
205 of 1 - 4.5 h (Mäki et al., 2017). To prevent the degradation of BVOC by O<sub>3</sub>, a catalyst heated to 150°C was used.

206 Individual VOCs were identified and quantified using a thermal desorption instrument (Perkin-Elmer  
207 TurboMatrix™ 650, Waltham, USA) connected to a gas chromatograph (Perkin-Elmer® Clarus® 600,  
208 Waltham, USA) with a DB-5MS (60 m, 0.25 mm, 1 μm) column and a mass selective detector (Perkin-Elmer®  
209 Clarus® 600T, Waltham, USA). Five-point calibration was utilised using liquid standards in methanol solutions.  
210 Standard solutions were injected onto adsorbent tubes that were flushed with nitrogen (HiQ N<sub>2</sub> 6.0 >99.9999%,  
211 Linde AG, Pullach, Germany) flow (100 ml min<sup>-1</sup>) for 10 min in order to remove methanol. For aromatic  
212 hydrocarbons (benzene, toluene, ethylbenzene, p/m-xylene, styrene, o-xylene, propylbenzene, ethyltoluenes,  
213 trimethylbenzenes) detection limits (LODs) varied between 5 and 60 ng m<sup>-3</sup>, for C<sub>6-10</sub> alkanes (hexane, heptane,  
214 octane, nonane, decane) between 5 and 10 ng m<sup>-3</sup> and for isoprene LOD was 21 ng m<sup>-3</sup>. The quantified  
215 monoterpenes (MT) were α-pinene, camphene, β-pinene, Δ<sup>3</sup>-carene, p-cymene, limonene, 1,8-cineol, nopinone,  
216 terpinolene and bornylacetate with limit of detection in the range of 3-17 ng m<sup>-3</sup>; sesquiterpenes were  
217 longicyclene, iso-longifolene, aromadendrene, β-caryophyllene and α-humulene with LOD of 20 ng m<sup>-3</sup>.

### 219 2.2.3 NMVOC PTR-MS Measurements

220 In addition to canister and cartridge samples, NMVOCs were continuously measured over time by a high-  
221 sensitivity proton transfer reaction mass spectrometer (PTR-MS, Ionicon, built in 2008) (Lindinger et al., 1993).  
222 In brief NMVOCs with a higher proton affinity than water vapor were charged via H<sub>3</sub>O<sup>+</sup> ions and subsequently  
223 mass selectively detected by applying a distinct electric field strength for the individual masses selected. More  
224 details on the techniques can be found elsewhere (Blake et al., 2009). In total, 72 selected NMVOCs were  
225 measured between June 11 and August 29, 2014 via a heated inlet (T = 60°C) at street level out of the street  
226 facing window of a measurement van (MW088) at approximately 2.5 m above surface. Note that this PTR-MS  
227 detected integer ion mass numbers only and no time of flight option was available for this version. Selection of  
228 masses were based on two aspects: first, typical mass to charge (m/z) ratios for anthropogenic and biogenic  
229 sources like benzene, toluene, isoprene and terpenes, and second, on mass scan results conducted once a week  
230 throughout the campaign period. In this way some masses changed during the total observation time because of  
231 changed scan intensities and the limited number of masses to be selected. Time resolution was set to 270 s, i.e.  
232 4.5 min. The dataset was averaged after the campaign for 30 min and 1h for comparison with other less time  
233 resolved measurement data. The drift tube pressure (p<sub>drift</sub>) was kept between 2.1 and 2.3 mbar with a mean of  
234 2.2 mbar. The detection chamber pressure was kept at 2x10<sup>-5</sup> mbar. The intensity of the reference ion signal for  
235 detection efficiency, i.e. m/z = 21, was recorded as (4.4±1.0)×10<sup>7</sup> counts per second. For more details on the set-  
236 up see Bourtsoukidis et al. (2014). A list of all recorded masses can be found in the supporting online  
237 information. Because the PTR-MS technique does not allow for a detailed chemical structure analysis, the  
238 cartridge and canister samples were used as complementary information as to the identity of masses with more  
239 than a single compound present.

### 241 2.2.4 Particle Number Concentration and Surface Area Measurements

242 The aerosol inlet was located 3.5 m above ground, about 1 m above the measurement van roof, attached  
243 to an aerosol splitter (Leibniz Institute for Tropospheric Research (TROPOS), “Kuh”). A LVS pump (Leckel

244 GmbH, Berlin) operated at  $1 \text{ m}^3 \text{ h}^{-1}$  corresponding to an aerosol flow of  $138 \text{ cm}^3 \text{ sec}^{-1}$  and a PM10-head (Leckel  
245 GmbH, Berlin) suitable for cut of at  $10 \text{ }\mu\text{m}$  with  $2.3 \text{ m}^3 \text{ h}^{-1}$  was used to reduce diffusion losses. This served all  
246 particle measurement instruments.

247 The instruments that measured particle number (PN) and particle size distribution included a GRIMM  
248 1.108 (particle sizes in optical equivalent diameter, GRIMM Aerosol Technik GmbH & Co. KG, Ainring),  
249 GRIMM 5.403, and GRIMM 5.416 (particle sizes in mobility equivalent diameter). Sampling average was  
250 mostly 1 min and 8 minutes for Grimm 5.403.

251 The GRIMM 5.416, a condensation particle counter with n-butanol, provided total PN count over a size  
252 range from 4-3000 nm at a flow rate of  $1.5 \text{ L min}^{-1}$ , and the uncertainty for 1 min sampling was  $\pm 0.1\%$  or  $\pm 15$   
253  $\text{cm}^{-3}$  (Helsper et al., 2008; Wiedensohler et al., 2017). The GRIMM 5.403, a scanning mobility particle sizer  
254 equipped with a long DMA combined with a CPC with n-butanol measured particle number concentrations with  
255 size distribution information for particles between 10-1100 nm at a sample flow rate of  $0.3 \text{ L min}^{-1}$  and a sheath  
256 flow rate of  $3 \text{ L min}^{-1}$ . For technical details see Heim et al., (2004). The uncertainty associated with the  
257 measurement is size dependent, with an uncertainty range of 10-15% in the lowermost size range and approx. 2-  
258 3% in the upper size range, and a total of 44 size bins. The GRIMM 1.108, a portable laser aerosol spectrometer  
259 and dust monitor measured particle number concentration with size distribution information, covering 350-22500  
260 nm, with a sampling flow rate of  $1.5 \text{ L min}^{-1}$ . Particle number concentrations were determined for 15 size bins  
261 with an uncertainty of  $\pm 3\%$ . For technical details see Görner et al. (2012).

262 The TSI Nanoparticle surface area monitor 3550 (NSAM) measured lung depositable surface area for  
263 particle sizes ranging from 10-1000 nm at a flow rate of  $2.5 \text{ L min}^{-1}$ . These values are reported in units of  $\mu\text{m}^2$   
264  $\text{cm}^{-3}$  corresponding to empirically derived parameters that correspond to the regions where the particles are  
265 deposited in the lung. Alveolar deposition was measured. Measurement accuracy for the NSAM was  $\pm 20\%$  for  
266 both parameters. Further instrument and measurement details are described elsewhere (Kaminski et al.,  
267 2013;VDI, 2017).

268 The NSAM was calibrated at the German Environment Agency (UBA, Langen) with instruments from  
269 IUTA, Duisburg (Kaminski, 2011), the GRIMM 1.108 was sent in for maintenance and re-calibrated at the  
270 manufacturer prior to use in the campaign, while all other instruments were calibrated a priori at the TROPOS  
271 aerosol calibration facility in Leipzig (Weinhold, 2014).

272 A continuous aerosol size distribution ( $0.01 \text{ }\mu\text{m}$  to  $30 \text{ }\mu\text{m}$ ) was created using a combination of GRIMM  
273 5.403 ( $0.01 \text{ }\mu\text{m}$  to  $1.1 \text{ }\mu\text{m}$ ) and GRIMM 1.108 ( $0.3 \text{ }\mu\text{m}$  to  $30 \text{ }\mu\text{m}$ ). Averaged 1-h size distribution from both  
274 particle instruments were merged to create a full size distribution from  $0.01$  to  $30 \text{ }\mu\text{m}$ . Size distributions from the  
275 two analyzers were merged by considering GRIMM 5.403 for particles sizes  $<1.1 \text{ }\mu\text{m}$  and sizes equal or above  
276  $1.1 \text{ }\mu\text{m}$  uses GRIMM 1.108. At  $1.1 \text{ }\mu\text{m}$  both individual logarithmic size bin boundaries of the 5.403, and 1.108  
277 were most similar allowing “a smooth merge” without losing any size bins. We also assumed that the particles  
278 were spherical and thus no adjustments were made in the size bins, nor were any adjustments made for possible  
279 differences in aerodynamic vs optical derivation of diameter.

280

### 281 2.2.5 Ceilometer

282 State-of-the-art ceilometers provide the vertical profile of aerosol backscatter (Wiegner et al., 2014).  
283 There are numerous approaches to estimate the mixing layer height (MLH) from the measured profile; the  
284 underlying assumption is that at the top of the mixing layer aerosol concentration drastically drops resulting in a

285 pronounced decrease of backscattered signal intensity. Measurements in the framework of BAERLIN2014 were  
286 performed with a Vaisala ceilometer CL51 (Münkel, 2007;Geiß et al., 2017). This instrument is eye-safe (class  
287 1M), operated fully automated and unattended. The diode laser emits at a wavelength of 910 nm; the absorption  
288 by water vapour can be ignored as long as only the MLH is to be determined (Wiegner and Gasteiger, 2015).  
289 Laser power and window contamination are permanently monitored to ensure long-term stability. Due to the one  
290 lens design the lowest detectable layers are around 50 m, and the system is capable to cover an altitude range  
291 greater than 4000 m, topping out around 8 km. Signals are pre-processed, e.g. for the suppression of noise  
292 generated artefacts. The range resolution is 10 m, and the temporal averaging is 10 min.

293 The heights of the near surface aerosol layers were analysed by a gradient method from the backscatter  
294 profiles in real-time (Emeis et al., 2008) with a MATLAB-based software which is provided by the manufacturer  
295 and has been improved continuously (Münkel et al., 2011). The minima of the vertical gradient is used to  
296 provide an estimate of the MLH (Emeis et al., 2007). All MLH data presented are following this method (for  
297 more detail see Schäfer et al. (2015)) unless otherwise noted. The influence of different options of the  
298 proprietary software and an comparison with the more sophisticated approach COBOLT (COntinuous BOundary  
299 Layer Tracing) on the retrieved MLH is discussed in detail by Geiß et al. (2017). It was found that the  
300 proprietary software slightly tends to overestimate the MLH compared to COBOLT.

301 The various instruments outlined above had differing sampling times and so for those instruments that  
302 provided real-time or higher time resolution data, a 30 minute average will be used in the data presented here for  
303 comparability.

304

#### 305 **2.2.6 PM<sub>10</sub> Filter Analysis**

306 Prior to sampling, the quartz fiber filters were baked at 800°C under synthetic air to remove impurities.  
307 Post-sampling, the PM<sub>10</sub> filters were analyzed for total mass, elemental carbon (EC), water soluble and total  
308 organic carbon, chloride, sulfate, nitrate, sodium, ammonium, potassium, calcium, and organic tracers.  
309 HYSPLIT back trajectories (based on GDAS meteorological data) were calculated for 72 hours over the time  
310 period of each filter with a new trajectory each 6 hours for air masses ending at ground level (at the monitoring  
311 station) (Stein et al., 2015). Back trajectory plots are included in the Supplemental Information following the  
312 final filter groups. Based on similarities in the bulk composition analysis and HYSPLIT back trajectory  
313 information, the filters were grouped before being extracted and analyzed for organic tracers. Not all filters were  
314 included in these groups, so as to create groups that showed significant similarities. Some individual filters were  
315 therefore also excluded from the organic tracer analysis because of a lack of remaining OC mass.

316 PM<sub>10</sub> mass was first quantified gravimetrically and then analyzed for elemental and organic carbon.  
317 For this the filter samples were heated to 750°C in an oxygen stream. The gas stream was then passed through an  
318 oxidation catalyst to ensure complete oxidation of the organic carbon to carbon dioxide (CO<sub>2</sub>). In contrast to the  
319 organic carbon, elemental carbon is directly oxidized at higher temperatures without the requirement of a  
320 catalyst. The organic carbon, as CO<sub>2</sub>, was then detected using a cavity ring-down spectrometer (Picarro Inc.).  
321 The distinction between the elemental and organic carbon fractions in the samples was based on the temperature  
322 profile during the analysis. For more details see Ehlers (2013) and Kofahl (2012).

323 A portion of the filter (1.5 cm<sup>2</sup>) was water extracted to determine water soluble organic carbon (WSOC)  
324 using a TOC-V SCH Shimadzu total organic carbon analyzer (Miyazaki et al., 2011;Yang et al., 2003). The  
325 remaining amount of OC was calculated as water insoluble organic carbon (WIOC). A fraction of the remaining



326 solution was used to analyze for water soluble anions and cations by ion chromatography (Dionex ICS 2100 and  
327 Dionex ICS 100) (Wang et al., 2005). For the organic tracer analysis, filters were composited as per the bulk  
328 composition and HYSPLIT determined groups and extracted with 50/50 dichloromethane and acetone by  
329 sonication, an aliquot was derivatized and analyzed by GC-MS (GC-6980, quadropole MS-5973, Agilent  
330 Technology) for organic molecular marker compounds, as described in more detail by Villalobos et al. (2015)  
331 and references therein. Approximately 150 organic tracer species were analyzed for, of which less than 100 had  
332 concentrations regularly above the detection limit. A limited subset of these was then used in the source  
333 apportionment analysis.

334

### 335 2.3 Chemical Mass Balance for Source Apportionment

336 A chemical mass balance analysis of the organic carbon fraction of the PM<sub>10</sub> filter samples was carried  
337 out using the organic tracer information. Source apportionment analysis using the CMB technique provides an  
338 effective variance least squares solution for a set of linear equations that include the uncertainties of the input  
339 measurements, and have been applied to the mass balance receptor model (Watson et al., 1984). As such, it  
340 allows for the estimation of the contribution of different source categories to the ambient concentrations  
341 measured at any one location, in this case an urban background site in Berlin. The species included in the CMB  
342 analysis were levoglucosan, 17 $\alpha$ (H)-21 $\beta$ (H)-30-norhopane, 17 $\alpha$ (H)-21 $\beta$ (H)-hopane, benzo(b)fluoranthene,  
343 benzo(k)fluoranthene, benzo(e)pyrene, benzo(a)pyrene, and C27-C33 alkanes. The US EPA CMB Software  
344 version 8.2 was used. Source profiles for vegetative detritus (Rogge et al., 1993), wood burning (Fine et al.,  
345 2004), diesel and gasoline motor vehicles (Lough et al., 2007) were included in the final result. In addition, a  
346 profile for poorly maintained vehicles ('smoking vehicles') (Lough et al., 2007) was evaluated but found  
347 inappropriate. The link between tracers and sources is discussed in further detail in section 3.5.2. The secondary  
348 organic aerosol fraction was calculated based on WSOC not related to biomass burning (Sannigrahi et al., 2006).  
349 The fitting statistics for the final result are shown in Table 3.

350

## 351 3 Results & Discussion

352

### 353 3.1 Time Series and Diurnal Cycle

354 The 30 min data time series of O<sub>3</sub>, NO<sub>2</sub>, NO, CO, benzene, toluene, and PM<sub>10</sub>, along with basic  
355 meteorological data from the BLUME station in Neukölln and MLH as derived from the proprietary software are  
356 shown in Figure 2, spanning the duration of the campaign. All times are given in CET. The 8 h mean ozone  
357 concentrations show that the EU target value for ozone (120  $\mu\text{g m}^{-3}$  based on 8 h means) was exceeded 6 times  
358 during the measurement period, and the WHO guideline (100  $\mu\text{g m}^{-3}$ ) was exceeded 18 times. The hourly limit  
359 value for NO<sub>2</sub> (200  $\mu\text{g m}^{-3}$ ) was not exceeded, though concentrations often exceeded 100  $\mu\text{g m}^{-3}$ . The daily limit  
360 value for PM<sub>10</sub> (50  $\mu\text{g m}^{-3}$ ) was not exceeded.

361 Elevated concentrations were often observed at the same time for many of the pollutants included in  
362 Figure 2, with the exception of ozone. Ozone, as a secondary pollutant formed photochemically from NO<sub>x</sub> and  
363 NMVOC precursors, follows a similar pattern to temperature (Pearson correlation coefficient [standard error] of  
364 0.82 [0.014]), and peaks at different times than the primary pollutants. The formation of ozone can be limited by  
365 either NO<sub>x</sub> or NMVOCs, depending on the ambient concentrations which are controlled by sources (e.g.,  
366 vehicles, biogenics) and transport. NO<sub>2</sub>, NO, CO, toluene, and benzene all have diurnal cycles that peak in the

367 morning and evening, reflecting their anthropogenic traffic-related emission sources (see Figure S1 in SI). The  
368 morning peak in the pollutants occurred at 7 or 8 am, while the evening peak occurred quite late between 9 and  
369 11 pm, likely owing to a combination of daytime emissions and the decrease in the MLH. Traffic counts, from  
370 MC143 and MC220 in Neukölln (see location in Figure 1), showed that traffic increased dramatically between 6  
371 and 8-9 am, after which a slow but steady increase led to a peak at 5-6 pm, after which the traffic count dropped  
372 dramatically. In contrast, ozone, temperature, and mixing layer height followed parallel diurnal cycles with a  
373 minimum at 6 am and a broad afternoon peak between noon and 6 pm. During BAERLIN2014 the maximum  
374 height of the mixing layer was found to be 1.5-2 km between noon and 18:00 and below 500 m during the  
375 night/early morning. These numbers indicate the vertical extent of the urban pollution layer over the  
376 measurement site where pollutants are most likely residing. Relative humidity showed the opposite with a peak  
377 at 6 am, and a broad low between noon and 6 pm.

378 These results are supported by the Pearson correlation coefficients among NO<sub>2</sub>, NO, CO, toluene, and  
379 benzene, which for hourly values range from 0.51-0.82 (all statistically significant at an alpha=0.05; see Table  
380 S2), with the strongest relationship between CO and NO<sub>2</sub>. The correlation to relative humidity was found to be  
381 negative for MLH (-0.66 [0.022]), temperature (-0.71 [0.014]), and ozone (-0.76 [0.014]). The pollutant with the  
382 strongest relationship to temperature was ozone.

383 The time series of particulate matter mass (PM<sub>10</sub>), derived PM<sub>1</sub>, PM<sub>2.5</sub>, and PM<sub>10</sub> mass from the  
384 GRIMM 1.108 particle number size distribution measurements, total particle number, and particle surface area  
385 are shown in Figure 3. While the two PM<sub>10</sub> time series along with the PM and particle number time series  
386 associated to the same instrument (GRIMM 1.108) are most similar, the other total particle number time series  
387 do not show significant similarities. This is largely owing to the difference in size fractions measured by the  
388 different instruments. Correlation analysis of the pollutant concentrations from Neukölln with MLH values on  
389 the basis of averaged diurnal cycles of hourly-mean values (in our case monthly averages during July and  
390 August) provided highest correlations with PN for accumulation mode particles (size range 100 – 500 nm) and  
391 significant correlations for PM<sub>2.5</sub> and PM<sub>1</sub> (Schäfer et al., 2015) showing similarities to investigations in  
392 Augsburg, Germany (Schäfer et al., 2016) and Beijing, China (Tang et al., 2016). In addition to this  
393 investigation for the reference site, a more detailed correlation analysis of the MLH with PM<sub>10</sub>, O<sub>3</sub>, and NO<sub>x</sub>  
394 taking into account all 16 BLUME stations in Berlin was carried out using the MATLAB approach outlined  
395 here, as well as an alternative approach, COBOLT (Geiß et al., 2017). In this context it was assumed that the  
396 MLH derived for the reference site in Neukölln is representative for the entire metropolitan area of Berlin. The  
397 correlation analysis of the diurnal cycles (averaged over the duration of ceilometer measurements from  
398 BAERLIN2014) of the MLH and PM<sub>10</sub> found that correlations were completely different at the different sites  
399 regardless of site type, indicating that surface concentrations of PM<sub>10</sub> were not predominantly determined by the  
400 MLH, but rather by local sources and sinks, and meteorological factors, among others. In the case of O<sub>3</sub>, strong  
401 positive correlations were identified for both the BLUME sites on the periphery of Berlin, as well as the urban  
402 background locations. In contrast, for NO<sub>2</sub>, a negative correlation to MLH was observed for all sites at the  
403 periphery of the city, and to a lesser extent at some of the urban background sites (Geiß et al., 2017).

404 Particle size distribution during the study period is shown in Figure 4. Size distribution was dominated  
405 by ultrafine number size distribution (“UFP”, <100 nm) throughout the day (i.e. particle formation close by). The  
406 number and volume distribution was further binned into at least 5 size bins, as presented in Figure 4 for  
407 comparison with other urban background measurements. The average daytime total number and volume

408 concentration remained in the range of  $5.5 - 6.0 \times 10^3 \text{ cm}^{-3}$  and  $11 - 12 \mu\text{m}^3 \text{ cm}^{-3}$ , respectively, in contrast to the  
409 stronger signal during the nighttime. The mean (median) total number and volume concentration over the entire  
410 measurement period was  $6.1 \times 10^3 \text{ cm}^{-3}$  ( $5.4 \times 10^3 \text{ cm}^{-3}$ ) and  $11.8 \mu\text{m}^3 \text{ cm}^{-3}$  ( $9.5 \mu\text{m}^3 \text{ cm}^{-3}$ ), respectively. Over  
411 80% of the total number concentration is ultrafine particles, and the contribution is higher during the nighttime.  
412 Volume distribution is largely dominated by the accumulation mode particles which is typical of many urban  
413 sites. The number concentrations were similar to other urban stations in Germany (Birmili et al., 2016).

414 The diurnal cycles for total PN for the three instruments covering the smaller particles (excluding the  
415 observations from the GRIMM-1.108) have morning and evening peaks, similar to the diurnal cycle for  $\text{NO}_2$ ,  
416 indicating a traffic origin. The diurnal cycle for the larger particles, as sampled by the GRIMM-1.108 has a much  
417 more dominant early morning peak and mid-afternoon minimum, without the second evening peak.

418 In Figure 5, at least two major contributors to UFP over the course of the day could be identified, in the  
419 morning and during the night. The presence of the morning peak is likely due to traffic-related emissions. Such a  
420 peak has also been identified in other species, as well as other studies in urban areas (Borsós et al.,  
421 2012; Mølgaard et al., 2013). There was a gradual increase in the UFP concentration from late afternoon which  
422 continues overnight till early morning hours. This nighttime feature of UFP was observed during weekends as  
423 well as on the weekdays. The reasons for this could be that the source contributing to this is something other than  
424 or in addition to traffic and may be active or enhanced overnight, the decrease in mixing layer height at night  
425 traps the particles in a smaller volume compared to daytime, and/or that night time deposition of particles is  
426 lower than daytime owing to higher atmospheric stability. The co-located trace gas measurement showed that the  
427 elevated UFP nighttime concentration correlates with toluene, among other gases such as CO. Daily  
428 observations also showed occasional and episodic “particle burst” (new particle formation) events for particles in  
429 the size range of 10-50 nm, which could be related to fresh plumes or to regional particle formation events.

430

### 431 **3.2 NMVOC measurements – Method comparison**

432 The results of the four NMVOC measurement methods were compared and contrasted for benzene and  
433 toluene. While differences in e.g., instrumentation and measurement technique (mass-to-charge (m/z) ratios vs  
434 compounds), inlet location, and time resolution, do not allow for direct comparisons, a comparison can be useful  
435 to understand how different or similar the information provided by the various methods can be. A summary of  
436 these methods and the compounds measured, including information on the detection limits and sampling times is  
437 provided in Table S1.

438 The 30-min data reported from the BLUME city air quality monitoring network was compared to the  
439 PTR-MS data for m/z 79 (benzene) and m/z 93 (toluene), as both instruments provide high time-resolution data.  
440 The correlations between the two methods were good given the imperfect nature of the comparison, both with  
441 Pearson’s r values for benzene and toluene of 0.39, significant at the  $p < 0.05$  level. The lower correlation values  
442 were likely owing to a number of factors including the differences in measurement method, and in location of the  
443 inlets for each instrument and thereby source influences – one of which (PTR-MS) was located on the street side  
444 of the van at approx. 2.5 m above ground, while the other (BLUME) was located above the measurement  
445 container approx. 5 m from the street. The inlet at the street would be influenced more directly by vehicle  
446 emissions in comparison to the inlet above the measurement container, which is especially relevant in that the  
447 PTR-MS was likely influenced by individual vehicles, while this would not be the case for the container  
448 measurements. This influence of vehicles on the PTRMS data at higher time resolution is supported by an

449 increase in Pearson's *r* values with longer averaging times, which reduces the influence of individual vehicles.  
450 For 1 h (3 h) average concentrations the *r* values increase to 0.48 (0.58) and 0.53 (0.71) for benzene and toluene,  
451 respectively, all significant at the  $p < 0.05$  level. Furthermore, the Pearson's *r* values for the correlations between  
452 the BLUME network and the individual canisters were 0.39 (benzene) and 0.83 (toluene), both statistically  
453 significant with  $p$ -values  $< 0.05$ , and between BLUME and the cartridge samples 0.51 (toluene) and not  
454 significant for benzene. All benzene and toluene measurements are shown in Figure S2.

455 In order to investigate the possibility of identifying molecular structures of PTR-MS derived *m/z*  
456 measurements, a comparison of the continuous measurements of the PTR-MS and intermittent canister samples  
457 was also carried out. For a number of cases only one compound quantified from the canister samples matched a  
458 specific *m/z*, while in other cases multiple compounds were quantified in the canister samples that had the same  
459 mass. For example, propanal, acetone, *n*-butane, and 2-methylpropane all have a molecular weight  
460 corresponding to *m/z* 59 (molar weight  $M_w = 58 \text{ g/mole} + M_w(\text{H}^+) = 1 \text{ g/mole}$ ), among which the PTR-MS  
461 cannot distinguish. In some cases, the fractional contribution of compounds with the same *m/z* ratio was  
462 relatively similar across all canister samples, as for *o*-xylene, *m+p*-xylene, and ethylbenzene (*m/z* 107). However  
463 this was rather the exception, with relative contributions more typically showing significant variation among the  
464 canister samples (see Figure S3 in the SI). Correlations between the canister samples and PTR-MS results were  
465 carried out for 35 individual *m/z* values for which at least one compound was quantified in the canister samples.  
466 While the absolute *r* values of the correlations ranged from 0.00016 to 0.63, the correlations were generally quite  
467 poor, showing little to no correlation for many of the *m/z* (only 9 of the 35 total number of *m/z* values evaluated  
468 had *r* values greater than 0.3), with no systematic bias identified. There are a number of reasons for this, beyond  
469 the difference in how the instruments measure (*m/z* vs compounds), such as inlet location and sampling time.  
470 Previously, in a targeted inter-comparison experiment where whole air samples (canisters) were compared with  
471 online PTR-MS measurements, differences of as little as 20 s in the sampling intervals contributed to scatter in  
472 the comparison of the two measurements that was especially relevant for the more reactive NMVOCs (de Gouw  
473 and Warneke, 2006). Additionally, scatter in inter-comparisons between ground-based fast time response and  
474 GC-MS systems was found to be typical (Lerner et al., 2017) and references therein). In the context of this study,  
475 the measurements should not be considered as an inter-comparison since, as described above, the inlets were  
476 approx. 5 meters apart, at different heights above ground level, with one street-side and the other above a  
477 measurement container. For these reasons, while both measurements are valid, as this comparison shows, the  
478 differences in quantification method, but also importantly instrument location and set-up result in substantial  
479 differences in what is being quantified so that the comparison is limited in value.

480

### 481 3.3 NMVOC Measurements – Characterization of different locations by canister sampling

482 The average fractional contribution to mixing ratio by compound class for each of the Neukölln,  
483 Altlandsberg, Plänterwald sites, the Tiergarten tunnel and the AVUS motorway samples is presented in Figure 6.  
484 The number of compounds included in each class was: alkanes (19), alkenes and alkynes (13), aromatics (14),  
485 oxygenated (6), and biogenics and their oxidation products (5; referred to as 'biogenics' for simplicity). For a  
486 complete list of the compounds and their grouping, see the supplemental information. In the following text and  
487 figures two extremely high values for acetone were removed (one sample from the Neukölln station, and one  
488 from the Altlandsberg samples). Since these two values were extreme outliers, their origin remains unclear.  
489 Therefore we have removed them from the averages and treated them separately. (Text is included in the SI to

490 demonstrate how these two values change the results presented here.) The largest contributions of the quantified  
491 VOCs to mixing ratio were from the alkanes (27 - 41 %) and oxygenated (23 - 55 %) compounds. Biogenics  
492 were always a minor contribution to mixing ratio, but their contribution was largest in the Plänterwald samples  
493 (11 %) and negligible at the two traffic locations. Alkenes/alkynes and aromatics showed the largest contribution  
494 to mixing ratio at the traffic sites, at 17 - 23 % and 14 %, respectively. The highest total NMVOC mixing ratio of  
495 those compounds measured here was found at the traffic sites (Tiergarten tunnel,  $64 \pm 17$  ppbv; AVUS  
496 motorway,  $170 \pm 82$  ppbv; average mixing ratio  $\pm$  standard deviation among the samples). The total mixing  
497 ratios of the 57 measured compounds at Altlandsberg and at the urban background station in Neukölln, showed  
498 similar results, with an average mixing ratio and standard deviation of  $14 \pm 6.4$  ppbv and  $19 \pm 5.6$  ppbv,  
499 respectively. The mixing ratios found in Plänterwald were similar to the urban background location, with an  
500 average of  $17 \pm 3.4$  ppbv, although with a larger contribution from biogenics. In comparison, total NMHC  
501 mixing ratios for urban background in Paris during the MEGAPOLI winter campaign was 12 ppbv (midnight  
502 median levels) or 17 ppbv (maximum of median daily values), with somewhat lower mixing ratios measured  
503 during the summer campaign (Dolgorouky et al., 2012; Ait-Helal et al., 2014).

504 Previously, a measurement campaign was carried out during June-August of 1996 in Berlin, during  
505 which samples were taken at the Neukölln urban background station, as well as at a traffic station on Frankfurter  
506 Allee. During this campaign, VOC measurements were taken 4 times a day for 2 hours over the course of one  
507 week (7 days) of each month using bag samples, adsorption tubes and DNPH cartridges and analyzed by gas-  
508 chromatography (Thijssse et al., 1999). This provides a good basis for comparison to the NMVOCs measured by  
509 canister sampling (most similar in method) during this campaign almost 20 years later. Overall, the mixing ratios  
510 for most compounds that were measured in both projects at the urban background location in Neukölln were  
511 lower now than in 1996 (Figure 7). For the traffic locations the results are less clear. Given that the Frankfurter  
512 Allee monitoring station is a traffic station, these measurements would likely be more comparable to the  
513 Tiergarten Tunnel measurements of this study, rather than those samples taken during a traffic jam on the AVUS  
514 motorway where concentrations were extremely elevated. Indeed, the mixing ratios measured during the traffic  
515 jam were found to be higher in most cases than those measured in 1996 at Frankfurter Allee. However, the  
516 comparison between the Tiergarten Tunnel measurements and Frankfurter Allee showed much more similar  
517 results to those of the urban background station comparison, with concentrations generally being lower today  
518 than approx. 20 years ago (Thijssse et al., 1999).

519 There are a couple of exceptions in this comparison, where the mixing ratios measured in this campaign  
520 stand out as substantially higher than those measured 20 years ago. Considering only those few compounds that  
521 have a ratio of 0.6 or less for the average mixing ratio in 1996 relative to that in 2014, the biogenic contributions  
522 in Neukölln (isoprene (0.3), methylvinylketone (0.1)) show increases. These increases may be attributable to  
523 changes in vegetation around the measurement site. Other NMVOCs, such as cis-2-butene and cyclopentane  
524 showed increases for both the urban background site and traffic site (Tiergarten Tunnel vs Frankfurter Allee).  
525 Other compounds, such as cis-2-pentene and trans-2-butene (traffic site) and 1,2,3-trimethylbenzene (urban  
526 background) showed increases at only the one site type. While the literature on trends of NMVOCs is limited,  
527 data from a traffic site in London, a rural background site in the UK, and a remote site in Germany showed that  
528 over the period from 1998-2009 all individual NMVOCs evaluated (with the exception of n-heptane at the rural  
529 background site) were decreasing, with stronger decreases observed at the traffic site relative to the other site  
530 types (von Schneidmesser et al., 2010). Similarly, an evaluation of C2-C8 hydrocarbon data, as total HCs and

531 by compound class, for a number of sites across the UK from 1994-2012, also documented decreases across all  
532 compound classes (Derwent et al., 2014). Finally, a broader evaluation of the trends in anthropogenic NMVOC  
533 emissions across Europe also documented a decrease between 2003 and 2012 (EEA, 2014, 2016). As such, the  
534 existing literature does not provide any detailed documentation that might be able to address the potential  
535 increases in those few compounds here where an increase was observed. Furthermore, longer-term sampling may  
536 show that the increases documented here do not reflect the long-term trend.

537

### 538 3.4 OH Reactivity

539 To better understand the role of these compounds with respect to their role in ozone formation and the  
540 reactivity of the measured compounds, the reactivity with respect to OH ( $R_{OH}$ ) was calculated. These results are  
541 shown in Figure 6 and parallel the results presented for the mixing ratios. In all cases, including other studies  
542 discussed, the values presented are calculated OH reactivity based on measurements of NMVOCs and not OH  
543 reactivity that was measured directly. Because the OH reactivity estimates are based on a limited number of  
544 NMVOCs, the values presented here are a lower limit. The relative importance of the biogenics, alkenes and  
545 alkynes, and to a lesser extent the aromatics increased when considering OH reactivity as is visible in Figure 6  
546 (for a complete list of compounds included in these classes, see the SI). The largest contribution to OH reactivity  
547 was from either the biogenics and their oxidation products (0-75%) or the alkenes and alkynes (10-55%),  
548 depending on the location, with the alkenes and alkynes dominating at the traffic locations, where the biogenic  
549 contribution was negligible. The NMVOCs included in each of these categories are provided in Section S1. The  
550 contribution to OH reactivity from alkanes ranged from 4% (Plänterwald) to 18% (AVUS motorway). The  
551 contribution from oxygenated compounds, despite their substantial contribution to mixing ratio, ranged from  
552 only 5-13% of OH reactivity. That said, only 6 oxygenated NMVOCs (of 57 total NMVOCs) were included  
553 here, and a recent study by Karl et al., (2018) found an appreciably greater fraction of oxygenated NMVOCs in  
554 urban areas than previous studies identified. The molar flux of oxygenated NMVOCs being actively emitted into  
555 the urban atmosphere from measurements in Europe was found to be  $56 \pm 10\%$  relative to the total NMVOC flux  
556 (Karl et al., 2018), which indicates that a much larger contribution from oxygenated NMVOCs is possible if  
557 different measurement techniques are used. The contribution to the biogenic OH reactivity at Plänterwald  
558 originated largely from isoprene (88%), with 7% from  $\alpha$ - and  $\beta$ -pinene. Similar contributions were found at  
559 Neukölln and Altlandsberg. The mean (median [25<sup>th</sup>, 75<sup>th</sup> percentile]) total OH reactivity from the 57 species  
560 was  $2.6 \text{ s}^{-1}$  ( $2.6 [2.1, 3.0] \text{ s}^{-1}$ ) at Neukölln, and ranged from  $2.2 \text{ s}^{-1}$  ( $2.2 [1.5, 2.8] \text{ s}^{-1}$ ) at Altlandsberg to  $34 \text{ s}^{-1}$  ( $34$   
561  $[29, 39] \text{ s}^{-1}$ ) from the AVUS motorway. While studies have shown that a number of NMVOCs, such as isoprene,  
562 or other terpenes can also have anthropogenic sources (Derwent et al., 2007;Reimann et al., 2000), we treat them  
563 as biogenic and do not try to tease apart the biogenic vs potential anthropogenic contributions in this context.

564 An earlier study (BERLIOZ) also made measurements of  $C_2$ - $C_{12}$  NMHCs in Berlin and at sites in the  
565 surrounding area, mostly focused on the production of ozone in downwind locations of the city (Winkler et al.,  
566 2002;Volz-Thomas et al., 2003;Becker et al., 2002). They report OH reactivity for two sites outside of Berlin,  
567 Blossin (approx. 15-20 km southeast of the Berlin city boundary) and Pabsthum (approx. 30-35 km northwest of  
568 the Berlin city boundary). The total OH reactivity reported at these sites range between  $1 - 7 \text{ sec}^{-1}$  and approx.  
569  $0.25 - 2 \text{ sec}^{-1}$ , respectively. These are similar to those values found at the urban background locations in Berlin,  
570 with the most comparable location being Altlandsberg ( $2.2 \text{ s}^{-1}$ ). The contribution from isoprene to the OH  
571 reactivity was found to be 70% at Blossin and 51% at Pabsthum, on average, although during the passing of a

572 city plume at Pabsthum 46% of reactivity was contributed by isoprene, with the remaining contribution  
573 attributed to anthropogenic NMHCs (Winkler et al., 2002).

574 The total OH reactivity values of measured VOCs in Berlin ( $2.6 \text{ s}^{-1}$ ) are similar to the average total OH  
575 reactivity from VOCs observed in other European cities, such as Paris (approx.  $4.0 \text{ s}^{-1}$ ) and London ( $1.8 \text{ s}^{-1}$ )  
576 (Dolgorouky et al., 2012; Whalley et al., 2016), and, not surprisingly, lower than those observed at cities in the  
577 Pearl River Delta region of China ( $8\text{-}14 \text{ s}^{-1}$ ). Specifically, Liu et al. (2008) reported OH reactivity from a  
578 measurement campaign in Ghangzhou and Xinken during one month in the autumn of 2004. The OH reactivity  
579 from alkanes, alkenes, and aromatics from Ghangzhou was reported to be  $1.9 \pm 1.5 \text{ s}^{-1}$ ,  $8.8 \pm 6.8 \text{ s}^{-1}$ , and  $2.9 \pm$   
580  $2.7 \text{ s}^{-1}$ , respectively. In all cases, these values are about one order of magnitude greater than those calculated for  
581 the urban background locations during this campaign (see Table 2). The level for isoprene ( $0.5 \pm 0.4 \text{ s}^{-1}$ )  
582 however, was much more similar to the OH reactivity reported for the biogenics at the urban background  
583 locations in this study. In London, OH reactivity of alkanes, alkenes+alkynes, aromatics, and biogenics was  
584 reported to be  $0.81 \text{ s}^{-1}$ ,  $0.47 \text{ s}^{-1}$ ,  $0.235 \text{ s}^{-1}$ , and  $0.25 \text{ s}^{-1}$ , respectively, which are values much more similar to those  
585 in this study (Whalley et al., 2016). The relative importance of alkanes and alkenes+alkynes was the reverse for  
586 London compared to Berlin.

587 In the MEGAPOLI winter campaign in Paris, total calculated mean OH reactivity was reported to be  
588  $17.5 \text{ s}^{-1}$ , although this included not only NMVOCs, but also methane, CO, NO, and  $\text{NO}_2$  (Dolgorouky et al.,  
589 2012). The OH reactivity attributed to the 29 non-methane hydrocarbons and oxygenated VOCs was 23% ( $4.0 \text{ s}^{-1}$ )  
590 of the total, somewhat higher than those values reported here (57 NMVOCs) for the urban background  
591 locations. Comparing to the OH reactivity values in Berlin is difficult, since for the winter campaign in Paris,  
592 Ait-Helal et al. (2014) report that the concentrations of the VOCs are generally shown to be lower during  
593 summer, specifically for many of the anthropogenic compounds, although this does vary by compound.  
594 Therefore, the OH reactivity values for Paris considered here should be considered an upper limit for the  
595 comparison with this study. The calculated mean OH reactivity attributed to NO and CO was  $1.75 \text{ s}^{-1}$  each, and  
596  $9.63 \text{ s}^{-1}$  for  $\text{NO}_2$  in Paris (Dolgorouky et al., 2012). By comparison, the mean OH reactivity calculated for  
597 August (to match the time during which the canister samples were taken at Neukölln) was  $0.58 \pm 1.2 \text{ s}^{-1}$  and  $0.87$   
598  $\pm 0.30 \text{ s}^{-1}$  for NO and CO, respectively, and  $4.5 \pm 3.0 \text{ s}^{-1}$  for  $\text{NO}_2$ , which is again, lower, as with the VOCs, but  
599 not unreasonable given the context of the comparison.

600 Finally, while the 57 NMVOCs included here to calculate OH reactivity were chosen to facilitate  
601 comparison to previous studies, a more exhaustive list could change the picture. For example, as mentioned  
602 above, the limited number of oxygenated NMVOCs measured would likely lessen the contributions of the other  
603 compound classes. As an example, adding six additional oxygenated NMVOCs (propanal, 2-butanol, 1-propanol,  
604 butanal, 1-butanol, pentanal) increased the total average OH reactivity between  $0.12 \text{ s}^{-1}$  (Plänterwald) to  $1.7 \text{ s}^{-1}$   
605 (AVUS Motorway). The percent contribution of these six oxygenated NMVOCs ranges between 2.5% and 9.3%  
606 of the new total OH reactivity. In contrast, a similar analysis that included three additional biogenic NMVOCs  
607 (limonene, sabinene, eucalyptol) showed much smaller additional reactivity, never more than  $0.02 \text{ s}^{-1}$ . These  
608 compounds also were not consistently present across all samples.

609

#### 610 **3.4.1 OH reactivity – direct comparison to a previous study in London and Paris**

611 As a comparison to the  $R_{\text{OH}}$  estimates calculated for London and Paris based on approx. 10 years of  
612 monitoring data through 2009 (von Schneidmesser et al., 2011), a subset of the NMVOCs was taken to enable a

613 more equal comparison to the values reported for summer (JJA) in that study. The only difference in the  
614 compounds included is the contribution of n-butane, which was not included in the Berlin calculations because  
615 of a local source of contamination (in London the contribution of n-butane to OH reactivity from this subset of  
616 NMVOCs was approx. 5% or less). The referenced study was focused on the contribution of biogenics,  
617 specifically isoprene, to OH reactivity. At the London Eltham site (urban background) isoprene contributed 25%  
618 to the OH reactivity for summer and 16% at Paris Les Halles, also an urban background location (24 total  
619 NMVOCs, including 9 alkanes, 9 alkenes/alkynes, 5 aromatics, 0 oxygenated, 1 biogenic) (von Schneidmesser  
620 et al., 2011). Using the reduced, matched set of compounds, isoprene accounts for 37% of OH reactivity at the  
621 Neukölln location on average, and as much as 82% at the Plänterwald (urban park) location in Berlin. The  
622 Neukölln urban background location values are a bit higher than those in London and Paris, although not  
623 dramatically different. The Plänterwald urban park location however, demonstrates the importance of such areas  
624 for the biogenic influence on OH reactivity, especially considering that even at Harwell, a rural background  
625 location west of London in the UK, isoprene contributes on average only 10% of OH reactivity. Although, as  
626 pointed out in the study, this is likely an underestimation of the biogenic importance given that only isoprene is  
627 included and for northerly regions other biogenics, such as monoterpenes may play a more important role (von  
628 Schneidmesser et al., 2011).

629

### 630 **3.5 PM<sub>10</sub> Filters**

#### 631 **3.5.1 Bulk composition and HYSPLIT back trajectories**

632 The PM<sub>10</sub> filters were analyzed for water soluble and water insoluble OC, EC, and ions. In addition,  
633 filter samples were grouped to ensure enough mass for analysis of organic molecular markers. The groups were  
634 informed by the bulk composition analysis results, including the ratio of water soluble to total OC and the ratio  
635 of ions to OC, and HYSPLIT back trajectories. Back trajectories were evaluated to provide information on the  
636 origin of the air masses and source-receptor relationships (Stein et al., 2015). The results of this bulk  
637 composition analysis are shown in Figure 8. Select individual filters that had sufficient mass and did not fit with  
638 any of the other groups were analyzed individually (B17, B19, B30). All values listed for groups are an average  
639 of the results from the filters included in the group. The air mass origins as per HYSPLIT are summarized in  
640 Table 3 (see also Figure S4).

641 Groups A, B, C, and D show significant similarity in their percent of OC that is WSOC, which ranges  
642 from 27 to 34%. The ratio of ions (sulfate, nitrate, ammonium) to OC is however, very different. Groups B and C  
643 have an ions:OC ratio of 1.2 and 0.98, while groups A and D have ratios of 0.56 and 0.50, respectively. The  
644 PM<sub>10</sub> mass loadings for B (20 µg m<sup>-3</sup>) and C (24 µg m<sup>-3</sup>) were lower than for A (27 µg m<sup>-3</sup>) and D (35 µg m<sup>-3</sup>),  
645 see Table 3. The concentrations of EC ranged between 1.1 and 1.9 µg m<sup>-3</sup> but did not group as with the other  
646 species, with the lowest concentration in group B and the highest in group C.

647 Group E had a very low percent of WSOC (19%) and an ions:OC ratio of 0.59. It also had the lowest  
648 PM<sub>10</sub> mass (20 µg m<sup>-3</sup>), and either the lowest or among the lowest concentrations for all ions. The OC  
649 concentration however, was 5.5 µg m<sup>-3</sup>, which was roughly in the middle of the OC concentrations measured,  
650 while the EC concentration was also the lowest at 0.71 µg m<sup>-3</sup>.

651 B17, B19, and B30 were analyzed individually because their bulk composition analysis and back  
652 trajectory patterns did not group well with the others, and sufficient mass was available for tracer analysis  
653 without needing to composite filters (Table 3, Figure 8). B17 and B30 had a higher percent WSOC (66% and



654 56%, respectively), and ions:OC ratios of 1.3 and 2.4, respectively. 37% of OC was WSOC for B19, and the  
655 ions:OC ratio was 0.77. Total PM<sub>10</sub> mass was 38.8 μg m<sup>-3</sup>, 31.0 μg m<sup>-3</sup>, and 39.5 μg m<sup>-3</sup>, and OC concentrations  
656 were 7.0 μg m<sup>-3</sup>, 5.9 μg m<sup>-3</sup>, and 3.9 μg m<sup>-3</sup>, for B17, B19, and B30, respectively. All three samples had  
657 significantly larger contributions from sulfate, and to a lesser extent also higher ammonium, compared to the  
658 other groups. B30 also has a large amount of nitrate in contrast to all other samples, and somewhat higher  
659 concentrations of potassium and sodium as well. B17 had the highest concentration of EC (2.3 μg m<sup>-3</sup>) of all  
660 samples.

661 There were significant concentrations of sulfate across all samples, ranging from 1.2-6.0 μg m<sup>-3</sup>, but  
662 particularly so in B17, B19, and B30. Sulfate is typically attributed to industrial sources, as the content of sulfate  
663 in fuels has been reduced significantly and is now quite low (Villalobos et al., 2015). Sea-salt is in this case not  
664 likely as a source, as Berlin is not within close proximity of a coastal region where such components are  
665 typically identified (Putaud et al., 2004). In general the significant contributions of sulfate, nitrate, and  
666 ammonium are indicative of a secondary inorganic aerosol (ammonium sulfate and ammonium nitrate) (Putaud  
667 et al., 2004;Schauer et al., 1996). Previous work has shown that secondary inorganic aerosol over northwestern  
668 Europe, including Germany, contribute significantly – about 50% – to the PM<sub>10</sub> concentrations (Banzhaf et al.,  
669 2013). Two studies by Putaud et al. (Putaud et al., 2004;Putaud et al., 2010) summarize the relative contribution  
670 of major constituent chemical species to PM mass, including for near-city and urban background locations. In  
671 comparison to the numbers cited in that study (2004 all European sites; 2010 north-western European sites), the  
672 percent contribution of nitrate (15%; 14%), ammonium (7%; not listed), and sulfate (13%; 14%) to PM<sub>10</sub> mass at  
673 the urban background site in Berlin were quite similar, ranging from 1-11% (nitrate), 1-5% (ammonium), and 6-  
674 16% (sulfate) in Berlin.

675 The back trajectories (Figure S4) show that prior to arriving in Berlin, the air masses primarily passed  
676 over Germany for group A. While some additional filters fit the general patterns outlined here, the number of  
677 filters included in the group was reduced to focus more on back trajectories in the group that originated from  
678 over Germany itself. The air masses that characterize group D originated from the Northeast, passing over the  
679 Baltic coast and Poland before arriving in Berlin. For group B the air masses originated from the West over the  
680 Atlantic (not further than 20 degrees W) and passed over northern France, the BeNeLux region and central  
681 Germany before arriving in Berlin. For group C, the air masses originated from the North West, over the North  
682 Sea as far as Iceland, passing between the UK and the Scandinavian Peninsula before arriving in Berlin. Both B  
683 and C had higher concentrations of sodium and nitrate than A and D, while A and D had higher concentrations of  
684 OC and marginally higher concentrations of sulfate than B and C (Figure 8). The air masses of Group E  
685 originated from the North, passing over Scandinavia, the North Sea, or the UK before arriving in Berlin. The  
686 back trajectories associated with B17 and B19 both passed over Poland before arriving in Berlin, with the air  
687 masses associated with B19 extending more northward as well. For B30 the air originates from the West with  
688 some passing over northern France, but mostly comes from over Germany itself. The significant presence of  
689 ammonium and sulfate likely indicates influence of agriculture, as ammonium sulfate is commonly used in  
690 fertilizer and more than 95% of NH<sub>3</sub> emissions in Europe originate from agriculture (Harrison and Webb,  
691 2001;Backes et al., 2016;EEA, 2016).

692

### 693 3.5.2 Organic molecular markers

694 The concentrations by composited sample are shown in Figure 9 for the organic molecular markers.  
695 Levoglucosan has been established as a molecular marker for biomass burning (Simoneit et al., 1999). The  
696 concentrations measured here ranged from 15-60 ng m<sup>-3</sup>. While high concentrations of levoglucosan in urban  
697 areas are often associated with residential wood combustion during colder months, it can also be owing to crop  
698 burning, wild fires, coal combustion and/or long-range transport of smoke from biomass burning (Simoneit,  
699 2002;Zhang et al., 2008;Shen et al., 2016). The concentrations measured during this summer campaign in Berlin  
700 were similar to those measured in PM<sub>10</sub> from other European cities during summertime, and approx. an order of  
701 magnitude lower than concentrations observed in winter (Caseiro and Oliveira (2012) and references therein).  
702 The study by Caseiro and Oliveira (2012) confirms the likelihood of agricultural residue burning and/or wildfires  
703 as a summertime source for levoglucosan.

704 Alkanes are useful tracers to distinguish between fossil fuel sources and vegetative detritus. This  
705 distinction is informed by the odd-even carbon number predominance, specifically of the C<sub>29</sub>, C<sub>31</sub>, and C<sub>33</sub> *n*-  
706 alkanes to indicate plant material as a source (Rogge et al., 1993). As is visible in Figure 9, the concentrations of  
707 those odd *n*-alkanes are much greater than the corresponding even *n*-alkanes. Furthermore, the carbon preference  
708 index (CPI) was calculated for the samples using the C<sub>29</sub>-C<sub>33</sub> *n*-alkanes and ranged from 1.9-5.5, with an average  
709 of 3.6. CPI values of approx. 1 are indicative of fossil fuel emission sources, whereas values of approx. 2 or  
710 greater are indicative of biogenic detritus (Simoneit, 1986), as is clearly the case for these samples.

711 Hopanes have been established as markers for diesel and gasoline vehicle emissions, stemming from  
712 petroleum product utilization and lubricating oil used in vehicles (Schauer et al., 1996;Rushdi et al.,  
713 2006;Simoneit, 1984). The concentrations of the two hopanes measured here and included in the CMB analysis  
714 ranged from 0.04-0.13 ng m<sup>-3</sup> as shown in Figure 9.

715 Polycyclic aromatic hydrocarbons (PAHs) are formed and emitted most typically during the incomplete  
716 combustion of fossil fuels or wood (Ravindra et al., 2008). The concentrations measured during this study ranged  
717 from 0-0.23 ng m<sup>-3</sup> for the individual PAHs shown in Figure 9. These concentrations are similar to, although on  
718 the lower end, of those measured in a study in Flanders, Belgium, including measurements at urban locations  
719 (Ravindra et al., 2006). Generally, PAH concentrations are lower in summertime owing to lower emissions and  
720 shorter lifetimes. The measurements here were conducted during summer, while the measurements in the study  
721 in Flanders covered more seasons. To distinguish between sources, PAH concentration profiles or ratios are  
722 used. For example, a ratio of benzo(b)fluoranthene to benzo(k)fluoranthene of greater than 0.5 has been  
723 identified as an indicator for diesel emissions sources (Park et al., 2002;Ravindra et al., 2008). In this study the  
724 ratio ranged from 1.9 to 7.2, indicating a strong influence of diesel emissions for these compounds.

725

### 726 3.5.3 Chemical Mass Balance

727 The molecular markers analyzed in the organic carbon fraction of the PM<sub>10</sub> samples were used to  
728 conduct source apportionment analysis using chemical mass balance. The total OC for these samples ranged  
729 from 2.99 to 7.21 µg m<sup>-3</sup>. The amount of OC mass apportioned in the CMB analysis ranged from 21% to 49%.  
730 The source profiles included in the model to which OC was attributed includes vegetative detritus, diesel  
731 emissions, gasoline vehicle emissions, and wood burning. In addition, a fraction of the unapportioned OC was  
732 attributed to secondary organic aerosol based on the unapportioned fraction of water soluble OC and the amount  
733 attributed to wood burning, following Sannigrahi et al. (2006). The source contributions to OC, as well as the  
734 fitting statistics are listed in Table 4, and shown in Figure 10.

735 For B17, B19, and B30 the SOA fraction is higher than for any of the others, at 63%, 34%, and 49% of  
736 OC, respectively. They also had the highest concentrations of levoglucosan, ranging from 37.8 to 60.1 ng m<sup>-3</sup>. As  
737 the primary tracer for biomass burning, these three samples also had the largest concentrations attributed to this  
738 source, ranging from 0.22 to 0.44 µg m<sup>-3</sup> of OC, but the relative contribution was only larger for B30 at 11%. All  
739 other samples had contributions that ranged between 2% and 4% of OC. These three samples had air masses that  
740 originated over Poland (B17, B19) and Germany (B30), indicating a more local-regional source for the biomass  
741 burning. The higher concentrations of potassium in these samples, also an indicator for biomass burning  
742 (Andreae, 1983), provides additional confirmation. The relatively high concentrations of ammonium and sulfate  
743 in these samples may indicate an agricultural influence. Those samples originating from regions to the  
744 West/North had somewhat lower concentrations overall relative to those originating from regions to the  
745 East/North, as shown in Figure 10.

746 The contribution of diesel emissions ranged from 0.24 - 0.81 µg m<sup>-3</sup>, corresponding to 4 - 21% of OC  
747 fraction. The highest fractional contribution was found in GRC (concentration 0.74 µg m<sup>-3</sup>) (air masses  
748 originating over the North Sea), while the highest concentration was found in sample B17 (fractional  
749 contribution 12%) (from Poland to the East). The diesel from GRC could also have its origin in shipping  
750 emissions, as well as diesel vehicles. High contributions of diesel did not necessarily correspond to high  
751 contributions of gasoline vehicle emissions, which were lower than the contributions from diesel and ranged  
752 from 0.11 - 0.28 µg m<sup>-3</sup> and 2 - 7% of OC. The highest contribution in terms of fractional contribution and  
753 concentration was found in B30. Furthermore, it should be noted that the source profiles reflect primary organic  
754 aerosol emissions, and therefore the secondary aerosol produced from these vehicular sources, which has been  
755 shown to be substantial in many cases, depending on the control technologies in use (Gordon et al.,  
756 2014a; Gordon et al., 2014b), is not reflected in these attributions.

757 The contribution of vegetative detritus was among the largest source contributions and ranged from 0.51  
758 - 1.4 µg m<sup>-3</sup> (11-20%). The relative importance of this source is reflected in the concentrations of the alkanes, as  
759 shown in Figure 9, and their average CPI of 3.6. The largest contribution was found for GRD with air masses  
760 originating over the North Sea.

761 For all samples, a significant amount of secondary organic aerosol was calculated, 0.87 - 4.4 µg m<sup>-3</sup> (18  
762 - 63%). While this was the contribution to OC, high concentrations of secondary inorganics (sulfate, ammonium,  
763 nitrate) support the aging of the air masses and the potential for a significant contribution from secondary aerosol  
764 overall.

765 It should be noted that ambient air samples include contributions from both local sources as well as  
766 emissions that have been transported from locations further away. While the back trajectory analysis is more  
767 relevant for interpreting the influence of emissions from the surrounding region, a comparison to the Berlin  
768 emission inventory reflects on the influence of local source contributions. Both play a role, but neither capture  
769 the complete picture, with limitations in both cases, as discussed further below.

770

#### 771 **3.5.4 Source apportionment – emission inventory comparison**

772 The source apportionment results were compared to the emissions inventory (EI) from TNO-MACC III  
773 (Kuenen et al., 2014). The grid cells for Berlin were extracted and the percent of total emissions for OC by  
774 source category for the Berlin area for June, July, and August as a rough comparison to the source apportionment  
775 results was calculated. Both diesel and gasoline vehicle exhaust sources have significant contributions, although

776 diesel contributes approx. 19% to total OC emissions in the inventory, whereas gasoline vehicles contribute only  
777 about 1%. Biogenic sources are not included in the inventory. If we focus on the primary sources from the source  
778 apportionment results, the diesel and gasoline vehicles contribute a significant fraction, with diesel comprising a  
779 larger fraction than gasoline vehicles, as in the inventory. The inventory also includes significant contributions  
780 from road transport originating from road, brake, and tire wear, which are not reflected in the CMB results,  
781 owing to the profiles used. About 8% of OC emissions are attributed to agriculture in the EI. This could  
782 contribute to both the biomass burning and vegetative detritus sources; the presence of significant secondary  
783 ammonium and nitrate also indicates an agricultural influence, even though this does not show up in the OC  
784 CMB. In all cases, these primary sources will contribute to secondary inorganic and organic aerosol formation.  
785 The contributions from non-industrial combustion and energy and other industries are not captured as primary  
786 source contributions in the CMB model. Overall, the comparison between the source apportionment results and  
787 the EI is a non-ideal comparison given the differences in methodology and the difference in terms of primary vs  
788 secondary sources that are or are not included. More specifically, the EI provides primary emissions estimates  
789 for a year for all Berlin grid cells (Kuenen et al., 2014), while the CMB results provide source attribution to  
790 ambient concentrations including primary and secondary sources for 3 months of summer at one location in  
791 Berlin. However, one would expect that general patterns are captured for significant sources, as it was for  
792 vehicle emissions, and the indication of agriculture.

793

#### 794 **4 Conclusions**

795 The data presented here provide an overview of the stationary measurements conducted during the  
796 BAERLIN2014 campaign. Of the three main aims of the campaign, two were addressed here, including (1)  
797 characterization of gaseous and particulate pollution, including source attribution, in the Berlin-Potsdam area, (2)  
798 quantification of the role of natural sources, especially vegetation, in determining levels of gaseous pollutants  
799 such as ozone.  $PM_{10}$  concentrations and the contributions from inorganic species, such as nitrate, sulfate, and  
800 ammonium that contribute substantially (10-24%) to secondary aerosol were found to be similar in terms of their  
801 relative contribution to  $PM_{10}$  in other European cities. Both the PM and gas-phase pollutants exhibited diurnal  
802 cycles indicative of anthropogenic sources, and the ratio of benzene to toluene indicated the influence of fresh,  
803 local emissions. Comparison of canister samples taken over the course of a day showed similarities which would  
804 seem to imply an urban background level for many NMVOC species. In addition to the secondary inorganic  
805 aerosol, a significant fraction of OC was attributed to secondary organic aerosol (18-63%) in the CMB analysis.

806 The influence of vegetation and biogenic emissions was demonstrated in the canister sample analysis, as  
807 well as the CMB results where vegetative detritus comprised one of the larger sources contributing to the OC  
808 fraction ranging from 11 to 20%. While the detected mixing ratios of the biogenic NMVOCs did not contribute  
809 significantly to the total NMVOC mixing ratio, the role in e.g., ozone formation, assessed by calculating OH  
810 reactivity, was much more significant. Biogenics and their oxidation products accounted for 31% of the OH  
811 reactivity at the urban background station in Neukölln and 75% at the urban park location (Plänterwald),  
812 demonstrating the importance of urban parks for biogenic emissions. These contributions from biogenics were  
813 higher than those found at comparable urban background locations in London and Paris. This is likely linked to  
814 the relatively high amount of land surface area in Berlin which is covered by vegetated areas (34%). It should  
815 however, be acknowledged that only a subset of the total NMVOCs were measured. If all 'missing' NMVOCs

816 were measured it could influence our results, including the contribution of biogenics and other compound classes  
817 to the calculated OH reactivity.

818 As an outlook, future research could build on this work to include additional analysis of PTR-MS data  
819 using positive matrix factorization to investigate the sources influencing NMVOC concentrations at the Neukölln  
820 location, as well as modeling studies to gain greater insight as to the impact of urban vegetation on ozone  
821 formation, both yielding further insight into the importance of biogenic VOCs in urban environments.

822

## 823 **5 Data availability**

824 The datasets generated during and/or analysed during the current study are available from the corresponding  
825 author on request.

826

## 827 **6 Acknowledgements**

828 This work was hosted by IASS Potsdam, with financial support provided by the Federal Ministry of Education  
829 and Research of Germany (BMBF) and the Ministry for Science, Research and Culture of the State of  
830 Brandenburg (MWFK). The authors would like to thank Hugo Denier van der Gon and Jeroen Kuenen (TNO)  
831 for providing information pertaining to the TNO-MACCIII inventory and Friderike Kuik for the Berlin  
832 emissions processing; Christoph Münkler from Vaisala GmbH, Hamburg for support with ceilometer CL51 data  
833 analyses to determine mixing layer heights; Wolfram Birmili (UBA), Alfred Wiedensohler, and Kay Weinhold  
834 (TROPOS) for discussions informing the particle measurements, colleagues at the IASS for their support of the  
835 campaign and discussions that helped shape the manuscript. The authors gratefully acknowledge the NOAA Air  
836 Resources Laboratory (ARL) for the provision of the HYSPLIT transport and dispersion model and/or READY  
837 website (<http://www.ready.noaa.gov>) used in this publication. Boris Bonn highly acknowledges a grant from the  
838 IASS to support the studies.

839

840

841

- 844 Ait-Helal, W., Borbon, A., Sauvage, S., de Gouw, J. A., Colomb, A., Gros, V., Freutel, F., Crippa, M., Afif,  
845 C., Baltensperger, U., Beekmann, M., Doussin, J. F., Durand-Jolibois, R., Fronval, I., Grand, N.,  
846 Leonardis, T., Lopez, M., Michoud, V., Miet, K., Perrier, S., Prévôt, A. S. H., Schneider, J., Siour, G.,  
847 Zapf, P., and Locoge, N.: Volatile and intermediate volatility organic compounds in suburban Paris:  
848 variability, origin and importance for SOA formation, *Atmos. Chem. Phys.*, 14, 10439-10464,  
849 10.5194/acp-14-10439-2014, 2014.
- 850 Andreae, M. O.: Soot carbon and excess fine potassium: long-range transport of combustion-derived  
851 aerosols, *Science (New York, N.Y.)*, 220, 1148-1151, 10.1126/science.220.4602.1148, 1983.
- 852 Backes, A. M., Aulinger, A., Bieser, J., Matthias, V., and Quante, M.: Ammonia emissions in Europe,  
853 part II: How ammonia emission abatement strategies affect secondary aerosols, *Atmos. Environ.*,  
854 126, 153-161, <http://dx.doi.org/10.1016/j.atmosenv.2015.11.039>, 2016.
- 855 Banzhaf, S., Schaap, M., Wichink Kruit, R. J., Denier van der Gon, H. A. C., Stern, R., and Builtjes, P. J.  
856 H.: Impact of emission changes on secondary inorganic aerosol episodes across Germany, *Atmos.*  
857 *Chem. Phys.*, 13, 11675-11693, 10.5194/acp-13-11675-2013, 2013.
- 858 Becker, A., Scherer, B., Memmesheimer, M., and Geiß, H.: Studying the city plume of Berlin on 20 July  
859 1998 with three different modelling approaches, *Journal of Atmospheric Chemistry*, 42, 41-70,  
860 10.1023/A:1015776331339, 2002.
- 861 Birmili, W., Weinhold, K., Rasch, F., Sonntag, A., Sun, J., Merkel, M., Wiedensohler, A., Bastian, S.,  
862 Schladitz, A., Löschau, G., Cyrus, J., Pitz, M., Gu, J., Kusch, T., Flentje, H., Quass, U., Kaminski, H.,  
863 Kuhlbusch, T. A. J., Meinhardt, F., Schwerin, A., Bath, O., Ries, L., Gerwig, H., Wirtz, K., and Fiebig, M.:  
864 Long-term observations of tropospheric particle number size distributions and equivalent black  
865 carbon mass concentrations in the German Ultrafine Aerosol Network (GUAN), *Earth Syst. Sci. Data*,  
866 8, 355-382, 10.5194/essd-8-355-2016, 2016.
- 867 Blake, R. S., Monks, P. S., and Ellis, A. M.: Proton-Transfer Reaction Mass Spectrometry, *Chemical*  
868 *Reviews*, 109, 861-896, 10.1021/cr800364q, 2009.
- 869 Bonn, B., von Schneidmesser, E., Andrich, D., Quedenau, J., Gerwig, H., Lüdecke, A., Kura, J., Pietsch,  
870 A., Ehlers, C., Klemp, D., Kofahl, C., Nothard, R., Kerschbaumer, A., Junkermann, W., Grote, R., Pohl,  
871 T., Weber, K., Lode, B., Schönberger, P., Churkina, G., Butler, T. M., and Lawrence, M. G.:  
872 BAERLIN2014 – the influence of land surface types on and the horizontal heterogeneity of air  
873 pollutant levels in Berlin, *Atmos. Chem. Phys.*, 16, 7785-7811, 10.5194/acp-16-7785-2016, 2016.
- 874 Borsós, T., Římnáčová, D., Ždímal, V., Smolík, J., Wagner, Z., Weidinger, T., Burkart, J., Steiner, G.,  
875 Reischl, G., Hitzemberger, R., Schwarz, J., and Salma, I.: Comparison of particulate number  
876 concentrations in three Central European capital cities, *Science of The Total Environment*, 433, 418-  
877 426, <http://dx.doi.org/10.1016/j.scitotenv.2012.06.052>, 2012.
- 878 Bourtsoukidis, E., Williams, J., Kesselmeier, J., Jacobi, S., and Bonn, B.: From emissions to ambient  
879 mixing ratios: Online seasonal field measurements of volatile organic compounds over a Norway  
880 spruce-dominated forest in central Germany, *Atmospheric Chemistry and Physics*, 14, 6495-6510,  
881 10.5194/acp-14-6495-2014, 2014.
- 882 Brauer, M., Freedman, G., Frostad, J., van Donkelaar, A., Martin, R. V., Dentener, F., Dingenen, R. v.,  
883 Estep, K., Amini, H., Apte, J. S., Balakrishnan, K., Barregard, L., Broday, D., Feigin, V., Ghosh, S., Hopke,  
884 P. K., Knibbs, L. D., Kokubo, Y., Liu, Y., Ma, S., Morawska, L., Sangrador, J. L. T., Shaddick, G.,  
885 Anderson, H. R., Vos, T., Forouzanfar, M. H., Burnett, R. T., and Cohen, A.: Ambient Air Pollution  
886 Exposure Estimation for the Global Burden of Disease 2013, *Environmental Science & Technology*, 50,  
887 79-88, 10.1021/acs.est.5b03709, 2016.

888 Caseiro, A., and Oliveira, C.: Variations in wood burning organic marker concentrations in the  
889 atmospheres of four European cities, *Journal of environmental monitoring : JEM*, 14, 2261-2269,  
890 10.1039/c2em10849f, 2012.

891 Colette, A., Bessagnet, B., Vautard, R., Szopa, S., Rao, S., Schucht, S., Klimont, Z., Menut, L., Clain, G.,  
892 Meleux, F., Curci, G., and Rouïl, L.: European atmosphere in 2050, a regional air quality and climate  
893 perspective under CMIP5 scenarios, *Atmos. Chem. Phys.*, 13, 7451-7471, 10.5194/acp-13-7451-2013,  
894 2013.

895 de Gouw, J., and Warneke, C.: Measurements of volatile organic compounds in the earth's  
896 atmosphere using proton-transfer-reaction mass spectrometry, *Mass Spectrometry Reviews*, 26, 223-  
897 257, 10.1002/mas.20119, 2006.

898 Derwent, R. G., Jenkin, M. E., Passant, N. R., and Pilling, M. J.: Photochemical ozone creation  
899 potentials (POCPs) for different emission sources of organic compounds under European conditions  
900 estimated with a Master Chemical Mechanism, *Atmos. Environ.*, 41, 2570-2579,  
901 <https://doi.org/10.1016/j.atmosenv.2006.11.019>, 2007.

902 Derwent, R. G.: New Directions: Prospects for regional ozone in north-west Europe, *Atmos. Environ.*,  
903 42, 1958-1960, 2008.

904 Derwent, R. G., Dorn, J. I. R., Dollard, G. J., Dumitrescu, P., Mitchell, R. F., Murrells, T. P., Telling, S.  
905 P., and Field, R. A.: Twenty years of continuous high time resolution volatile organic compound  
906 monitoring in the United Kingdom from 1993 to 2012, *Atmos. Environ.*, 99, 239-247,  
907 <https://doi.org/10.1016/j.atmosenv.2014.10.001>, 2014.

908 Dolgorouky, C., Gros, V., Sarda-Estevé, R., Sinha, V., Williams, J., Marchand, N., Sauvage, S., Poulain,  
909 L., Sciare, J., and Bonsang, B.: Total OH reactivity measurements in Paris during the 2010 MEGAPOLI  
910 winter campaign, *Atmos. Chem. Phys.*, 12, 9593-9612, 10.5194/acp-12-9593-2012, 2012.

911 EC: Directive 2008/50/EC of the European Parliament and of the Council of 21 May 2008 on ambient  
912 air quality and cleaner air for Europe, in: 2008/50/EC, edited by: Union, E. P. a. t. C. o. t. E., Official  
913 Journal of the European Union, 2008.

914 EEA: Air quality in Europe - 2014 report, European Environment Agency, Luxembourg, 2014.

915 EEA: Air quality in Europe - 2016 report, European Environment Agency, Luxembourg, 2016.

916 Ehlers, C.: Mobile Messungen: Messung und Bewertung von Verkehrsemissionen, PhD,  
917 Mathematisch-Naturwissenschaftliche Fakultät, Universität Köln, 2013.

918 Ehlers, C., Klemp, D., Rohrer, F., Mihelcic, D., Wegener, R., Kiendler-Scharr, A., and Wahner, A.:  
919 Twenty years of ambient observations of nitrogen oxides and specified hydrocarbons in air masses  
920 dominated by traffic emissions in Germany, *Faraday Discussions*, 189, 407-437,  
921 10.1039/C5FD00180C, 2016.

922 Emeis, S., Jahn, C., Münkel, C., Münsterer, C., and Schäfer, K.: Multiple atmospheric layering and  
923 mixing-layer height in the Inn valley observed by remote sensing, *Meteorologische Zeitschrift*, 16,  
924 415-424, 10.1127/0941-2948/2007/0203, 2007.

925 Emeis, S., Schäfer, K., and Münkel, C.: Surface-based remote sensing of the mixing-layer height a  
926 review, *Meteorologische Zeitschrift*, 17, 621-630, 10.1127/0941-2948/2008/0312, 2008.

927 Fine, P. M., Cass, G. R., and Simoneit, B. R. T.: Chemical Characterization of Fine Particle Emissions  
928 from the Fireplace Combustion of Wood Types Grown in the Midwestern and Western United States,  
929 *Environmental Engineering Science*, 21, 387-409, 10.1089/109287504323067021, 2004.

930 Geels, C., Andersson, C., Hänninen, O., Lansø, A., Schwarze, P., Skjøth, C., and Brandt, J.: Future  
931 Premature Mortality Due to O<sub>3</sub>, Secondary Inorganic Aerosols and Primary PM in Europe —  
932 Sensitivity to Changes in Climate, Anthropogenic Emissions, Population and Building Stock,  
933 *International Journal of Environmental Research and Public Health*, 12, 2837, 2015.

934 Geiß, A., Wiegner, M., Bonn, B., Schäfer, K., Forkel, R., von Schneidmesser, E., Münkel, C., Chan, K.  
935 L., and Nothard, R.: Mixing layer height as an indicator for urban air quality?, *Atmospheric*  
936 *Measurement Techniques*, 10, 2969-2988, 10.5194/amt-10-2969-2017, 2017.

937 Gilman, J. B., Kuster, W. C., Goldan, P. D., Herndon, S. C., Zahniser, M. S., Tucker, S. C., Brewer, W. A.,  
938 Lerner, B. M., Williams, E. J., Harley, R. A., Fehsenfeld, F. C., Warneke, C., and de Gouw, J. A.:  
939 Measurements of volatile organic compounds during the 2006 TexAQS/GoMACCS campaign:  
940 Industrial influences, regional characteristics, and diurnal dependencies of the OH reactivity, *Journal*  
941 *of Geophysical Research: Atmospheres*, 114, n/a-n/a, 10.1029/2008JD011525, 2009.

942 Goldan, P. D., Kuster, W. C., Williams, E., Murphy, P. C., Fehsenfeld, F. C., and Meagher, J.:  
943 Nonmethane hydrocarbon and oxy hydrocarbon measurements during the 2002 New England Air  
944 Quality Study, *J. Geophys. Res.*, 109, D21309, doi:10.1029/2003JD004455, 2004.

945 Gordon, T. D., Presto, A. A., May, A. A., Nguyen, N. T., Lipsky, E. M., Donahue, N. M., Gutierrez, A.,  
946 Zhang, M., Maddox, C., Rieger, P., Chattopadhyay, S., Maldonado, H., Maricq, M. M., and Robinson,  
947 A. L.: Secondary organic aerosol formation exceeds primary particulate matter emissions for light-  
948 duty gasoline vehicles, *Atmos. Chem. Phys.*, 14, 4661-4678, 10.5194/acp-14-4661-2014, 2014a.

949 Gordon, T. D., Presto, A. A., Nguyen, N. T., Robertson, W. H., Na, K., Sahay, K. N., Zhang, M., Maddox,  
950 C., Rieger, P., Chattopadhyay, S., Maldonado, H., Maricq, M. M., and Robinson, A. L.: Secondary  
951 organic aerosol production from diesel vehicle exhaust: impact of aftertreatment, fuel chemistry and  
952 driving cycle, *Atmos. Chem. Phys.*, 14, 4643-4659, 10.5194/acp-14-4643-2014, 2014b.

953 Görner, P., Simon, X., Bémer, D., and Lidén, G.: Workplace aerosol mass concentration measurement  
954 using optical particle counters, *Journal of Environmental Monitoring*, 14, 420-428, 2012.

955 Harrison, R., and Webb, J.: A review of the effect of N fertilizer type on gaseous emissions, in:  
956 *Advances in Agronomy*, Academic Press, 65-108, 2001.

957 Heim, M., Kasper, G., Reischl, G. P., and Gerhart, C.: Performance of a New Commercial Electrical  
958 Mobility Spectrometer, *Aerosol Science and Technology*, 38, 3-14, 10.1080/02786820490519252,  
959 2004.

960 Helsper, C., Horn, H.-G., Schneider, F., Wehner, B., and Wiedensohler, A.: Intercomparison of five  
961 mobility size spectrometers for measuring atmospheric submicrometer aerosol particles,  
962 *Partikelmessstechnik*, 68, 475-481, 2008.

963 Hengst, M.: Flüchtige Organische Verbindungen in der Ausatemluft von Kindern und Jugendlichen mit  
964 Asthma Bronchiale, PhD, Medizinischen Fakultät, Rheinisch-Westfälischen Technischen Hochschule  
965 Aachen, Aachen, Deutschland, 2007.

966 Jacob, D. J., and Winner, D. A.: Effect of climate change on air quality, *Atmos. Environ.*, 43, 51-63,  
967 10.1016/j.atmosenv.2008.09.051, 2009.

968 Kaminski, H.: personal communication, in, edited by: Gerwig, H., 2011.

969 Kaminski, H., Kuhlbusch, T. A. J., Rath, S., Götz, U., Sprenger, M., Wels, D., Polloczek, J., Bachmann, V.,  
970 Dziurawitz, N., Kiesling, H.-J., Schwiegelshohn, A., Monz, C., Dahmann, D., and Asbach, C.:  
971 Comparability of mobility particle sizers and diffusion chargers, *Journal of Aerosol Science*, 57, 156-  
972 178, <http://dx.doi.org/10.1016/j.jaerosci.2012.10.008>, 2013.

973 Karl, T., Striednig, M., Graus, M., Hammerle, A., and Wohlfahrt, G.: Urban flux measurements reveal a  
974 large pool of oxygenated volatile organic compound emissions, *Proceedings of the National Academy*  
975 *of Sciences*, 2018.

976 Kofahl, C.: Hochempfindliche Bestimmung der organischen und anorganischen Kohlenstoff-Fraktion  
977 in Feinstaubproben mittels CRD-Spektroskopie, BS, Chemie und Biotechnologie, Fachhochschule  
978 Aachen, 2012.



979 Kuenen, J. J. P., Visschedijk, A. J. H., Jozwicka, M., and Denier van der Gon, H. A. C.: TNO-MACC\_II  
980 emission inventory; a multi-year (2003–2009) consistent high-resolution European emission inventory  
981 for air quality modelling, *Atmos. Chem. Phys.*, 14, 10963–10976, 10.5194/acp-14-10963-2014, 2014.

982 Lelieveld, J., Evans, J. S., Fnais, M., Giannadaki, D., and Pozzer, A.: The contribution of outdoor air  
983 pollution sources to premature mortality on a global scale, *Nature*, 525, 367–371,  
984 10.1038/nature15371, 2015.

985 Lerner, B. M., Gilman, J. B., Aikin, K. C., Atlas, E. L., Goldan, P. D., Graus, M., Hendershot, R.,  
986 Isaacman-VanWertz, G. A., Koss, A., Kuster, W. C., Lueb, R. A., McLaughlin, R. J., Peischl, J., Sueper, D.,  
987 Ryerson, T. B., Tokarek, T. W., Warneke, C., Yuan, B., and de Gouw, J. A.: An improved, automated  
988 whole air sampler and gas chromatography mass spectrometry analysis system for volatile organic  
989 compounds in the atmosphere, *Atmos. Meas. Tech.*, 10, 291–313, 10.5194/amt-10-291-2017, 2017.

990 Lindinger, W., Hirber, J., and Paretzke, H.: An ion/molecule-reaction mass spectrometer used for on-  
991 line trace gas analysis, *International Journal of Mass Spectrometry and Ion Processes*, 129, 79–88,  
992 [http://dx.doi.org/10.1016/0168-1176\(93\)87031-M](http://dx.doi.org/10.1016/0168-1176(93)87031-M), 1993.

993 Liu, Y., Shao, M., Lu, S., Chang, C. C., Wang, J. L., and Chen, G.: Volatile Organic Compound (VOC)  
994 measurements in the Pearl River Delta (PRD) region, China, *Atmos. Chem. Phys.*, 8, 1531–1545,  
995 10.5194/acp-8-1531-2008, 2008.

996 Lough, G. C., Christensen, C. G., Schauer, J. J., Tortorelli, J., Mani, E., Lawson, D. R., Clark, N. N., and  
997 Gabele, P. A.: Development of molecular marker source profiles for emissions from on-road gasoline  
998 and diesel vehicle fleets, *Journal of the Air & Waste Management Association (1995)*, 57, 1190–1199,  
999 2007.

1000 Mäki, M., Heinonsalo, J., Hellén, H., and Bäck, J.: Contribution of understorey vegetation and soil  
1001 processes to boreal forest isoprenoid exchange, *Biogeosciences*, 14, 1055–1073, 10.5194/bg-14-  
1002 1055-2017, 2017.

1003 McDonald, B. C., de Gouw, J. A., Gilman, J. B., Jathar, S. H., Akherati, A., Cappa, C. D., Jimenez, J. L.,  
1004 Lee-Taylor, J., Hayes, P. L., McKeen, S. A., Cui, Y. Y., Kim, S.-W., Gentner, D. R., Isaacman-VanWertz,  
1005 G., Goldstein, A. H., Harley, R. A., Frost, G. J., Roberts, J. M., Ryerson, T. B., and Trainer, M.: Volatile  
1006 chemical products emerging as largest petrochemical source of urban organic emissions, *Science*  
1007 (New York, N.Y.), 359, 760, 2018.

1008 Miyazaki, Y., Kawamura, K., Jung, J., Furutani, H., and Uematsu, M.: Latitudinal distributions of  
1009 organic nitrogen and organic carbon in marine aerosols over the western North Pacific, *Atmos. Chem.*  
1010 *Phys.*, 11, 3037–3049, 10.5194/acp-11-3037-2011, 2011.

1011 Mølgaard, B., Birmili, W., Clifford, S., Massling, A., Eleftheriadis, K., Norman, M., Vratolis, S., Wehner,  
1012 B., Corander, J., Hämeri, K., and Hussein, T.: Evaluation of a statistical forecast model for size-  
1013 fractionated urban particle number concentrations using data from five European cities, *Journal of*  
1014 *Aerosol Science*, 66, 96–110, <http://dx.doi.org/10.1016/j.jaerosci.2013.08.012>, 2013.

1015 Münkel, C.: Mixing height determination with lidar ceilometers results from Helsinki Testbed,  
1016 *Meteorologische Zeitschrift*, 16, 451–459, 10.1127/0941-2948/2007/0221, 2007.

1017 Münkel, C., Schäfer, K., and Emeis, S.: Adding confidence levels and error bars to mixing layer heights  
1018 detected by ceilometer, 2011, 817708–817708–817709.

1019 Park, S. S., Kim, Y. J., and Kang, C. H.: Atmospheric polycyclic aromatic hydrocarbons in Seoul, Korea,  
1020 *Atmos. Environ.*, 36, 2917–2924, [http://dx.doi.org/10.1016/S1352-2310\(02\)00206-6](http://dx.doi.org/10.1016/S1352-2310(02)00206-6), 2002.

1021 Putaud, J.-P., Raes, F., Van Dingenen, R., Brüggemann, E., Facchini, M. C., Decesari, S., Fuzzi, S.,  
1022 Gehrig, R., Hüglin, C., Laj, P., Lorbeer, G., Maenhaut, W., Mihalopoulos, N., Müller, K., Querol, X.,  
1023 Rodriguez, S., Schneider, J., Spindler, G., Brink, H. t., Tørseth, K., and Wiedensohler, A.: A European  
1024 aerosol phenomenology—2: chemical characteristics of particulate matter at kerbside, urban, rural

- 1025 and background sites in Europe, *Atmos. Environ.*, 38, 2579-2595,  
1026 <http://dx.doi.org/10.1016/j.atmosenv.2004.01.041>, 2004.
- 1027 Putaud, J. P., Van Dingenen, R., Alastuey, A., Bauer, H., Birmili, W., Cyrys, J., Flentje, H., Fuzzi, S.,  
1028 Gehrig, R., Hansson, H. C., Harrison, R. M., Herrmann, H., Hitztenberger, R., Hüglin, C., Jones, A. M.,  
1029 Kasper-Giebl, A., Kiss, G., Kousa, A., Kuhlbusch, T. A. J., Löschau, G., Maenhaut, W., Molnar, A.,  
1030 Moreno, T., Pekkanen, J., Perrino, C., Pitz, M., Puxbaum, H., Querol, X., Rodriguez, S., Salma, I.,  
1031 Schwarz, J., Smolik, J., Schneider, J., Spindler, G., ten Brink, H., Tursic, J., Viana, M., Wiedensohler, A.,  
1032 and Raes, F.: A European aerosol phenomenology – 3: Physical and chemical characteristics of  
1033 particulate matter from 60 rural, urban, and kerbside sites across Europe, *Atmos. Environ.*, 44, 1308-  
1034 1320, <http://dx.doi.org/10.1016/j.atmosenv.2009.12.011>, 2010.
- 1035 Rasmussen, D. J., Hu, J. L., Mahmud, A., and Kleeman, M. J.: The Ozone-Climate Penalty: Past,  
1036 Present, and Future, *Environmental Science & Technology*, 47, 14258-14266, 10.1021/es403446m,  
1037 2013.
- 1038 Ravindra, K., Bencs, L., Wauters, E., de Hoog, J., Deutsch, F., Roekens, E., Bleux, N., Berghmans, P.,  
1039 and Van Grieken, R.: Seasonal and site-specific variation in vapour and aerosol phase PAHs over  
1040 Flanders (Belgium) and their relation with anthropogenic activities, *Atmos. Environ.*, 40, 771-785,  
1041 <http://dx.doi.org/10.1016/j.atmosenv.2005.10.011>, 2006.
- 1042 Ravindra, K., Sokhi, R., and Van Grieken, R.: Atmospheric polycyclic aromatic hydrocarbons: Source  
1043 attribution, emission factors and regulation, *Atmos. Environ.*, 42, 2895-2921,  
1044 <http://dx.doi.org/10.1016/j.atmosenv.2007.12.010>, 2008.
- 1045 Reimann, S., Calanca, P., and Hofer, P.: The anthropogenic contribution to isoprene concentrations in  
1046 a rural atmosphere, *Atmos. Environ.*, 34, 109-115, [https://doi.org/10.1016/S1352-2310\(99\)00285-X](https://doi.org/10.1016/S1352-2310(99)00285-X),  
1047 2000.
- 1048 Rogge, W. F., Hildemann, L. M., Mazurek, M. A., Cass, G. R., and Simoneit, B. R. T.: Sources of fine  
1049 organic aerosol. 4. Particulate abrasion products from leaf surfaces of urban plants, *Environmental  
1050 Science & Technology*, 27, 2700-2711, 10.1021/es00049a008, 1993.
- 1051 Rushdi, A. I., Al-Zarban, S., and Simoneit, B. R.: Chemical compositions and sources of organic matter  
1052 in fine particles of soils and sands from the vicinity of Kuwait city, *Environ Monit Assess*, 120, 537-  
1053 557, 10.1007/s10661-005-9102-8, 2006.
- 1054 Sannigrahi, P., Sullivan, A. P., Weber, R. J., and Ingall, E. D.: Characterization of Water-Soluble Organic  
1055 Carbon in Urban Atmospheric Aerosols Using Solid-State <sup>13</sup>C NMR Spectroscopy, *Environmental  
1056 Science & Technology*, 40, 666-672, 10.1021/es051150j, 2006.
- 1057 Schäfer, K., Blumenstock, T., Bonn, B., Gerwig, H., Hase, F., Münkel, C., Nothard, R., and  
1058 Schneidmesser, E. v.: Mixing layer height measurements determines influence of meteorology on  
1059 air pollutant concentrations in urban area, in: *Remote Sensing of Clouds and the Atmosphere XX*,  
1060 edited by: Comerón, A., Kassianov, E. I., and Schäfer, K., Proceedings of SPIE, Bellingham, WA, USA,  
1061 2015.
- 1062 Schäfer, K., Elsasser, M., Arteaga-Salas, J. M., Gu, J. W., Pitz, M., Schnelle-Kreis, J., Cyrys, J., Emeis, S.,  
1063 Prévôt, A. S. H., and Zimmermann, R.: Impact of meteorological conditions on airborne fine particle  
1064 composition and secondary pollutant characteristics in urban area during winter-time,  
1065 *Meteorologische Zeitschrift*, 25, 267-279, 2016.
- 1066 Schauer, J. J., Rogge, W. F., Hildemann, L. M., Mazurek, M. A., Cass, G. R., and Simoneit, B. R. T.:  
1067 Source apportionment of airborne particulate matter using organic compounds as tracers, *Atmos.  
1068 Environ.*, 30, 3837-3855, [http://dx.doi.org/10.1016/1352-2310\(96\)00085-4](http://dx.doi.org/10.1016/1352-2310(96)00085-4), 1996.
- 1069 Senatsverwaltung für Stadtentwicklung III F, B.: Informationssystem Stadt und Umwelt,  
1070 Flächennutzung und Stadtstruktur, Dokumentation der Kartiereinheiten und Aktualisierung des  
1071 Datenbestandes, Berlin Senatsverwaltung für Stadtentwicklung, Berlin, 2010.

- 1072 Shen, R., Schäfer, K., Schnelle-Kreis, J., Shao, L., Norra, S., Kramar, U., Michalke, B., Abbaszade, G.,  
 1073 Streibel, T., Fricker, M., Chen, Y., Zimmermann, R., Emeis, S., and Schmid, H. P.: Characteristics and  
 1074 sources of PM in seasonal perspective – A case study from one year continuously sampling in Beijing,  
 1075 Atmospheric Pollution Research, 7, 235-248, <http://dx.doi.org/10.1016/j.apr.2015.09.008>, 2016.
- 1076 Simoneit, B. R. T.: Organic matter of the troposphere—III. Characterization and sources of petroleum  
 1077 and pyrogenic residues in aerosols over the western united states, Atmospheric Environment (1967),  
 1078 18, 51-67, [http://dx.doi.org/10.1016/0004-6981\(84\)90228-2](http://dx.doi.org/10.1016/0004-6981(84)90228-2), 1984.
- 1079 Simoneit, B. R. T.: Characterization of Organic Constituents in Aerosols in Relation to Their Origin and  
 1080 Transport: A Review, International Journal of Environmental Analytical Chemistry, 23, 207-237,  
 1081 10.1080/03067318608076446, 1986.
- 1082 Simoneit, B. R. T., Schauer, J. J., Nolte, C. G., Oros, D. R., Elias, V. O., Fraser, M. P., Rogge, W. F., and  
 1083 Cass, G. R.: Levoglucosan, a tracer for cellulose in biomass burning and atmospheric particles, Atmos.  
 1084 Environ., 33, 173-182, [http://dx.doi.org/10.1016/S1352-2310\(98\)00145-9](http://dx.doi.org/10.1016/S1352-2310(98)00145-9), 1999.
- 1085 Simoneit, B. R. T.: Biomass burning — a review of organic tracers for smoke from incomplete  
 1086 combustion, Applied Geochemistry, 17, 129-162, [http://dx.doi.org/10.1016/S0883-2927\(01\)00061-0](http://dx.doi.org/10.1016/S0883-2927(01)00061-0),  
 1087 2002.
- 1088 Stein, A. F., Draxler, R. R., Rolph, G. D., Stunder, B. J. B., Cohen, M. D., and Ngan, F.: NOAA's HYSPLIT  
 1089 Atmospheric Transport and Dispersion Modeling System, Bulletin of the American Meteorological  
 1090 Society, 96, 2059-2077, 10.1175/bams-d-14-00110.1, 2015.
- 1091 Stülpnagel, A. v., Kaupp, H., Nothard, R., Preuß, J., Preuß, M., Clemen, S., and Grunow, K.:  
 1092 Luftgütemessdaten 2014, Senatsverwaltung für Stadtentwicklung und Umwelt, Berlin, 2015.
- 1093 Tang, G., Zhang, J., Zhu, X., Song, T., Münkel, C., Hu, B., Schäfer, K., Liu, Z., Zhang, J., Wang, L., Xin, J.,  
 1094 Suppan, P., and Wang, Y.: Mixing layer height and its implications for air pollution over Beijing, China,  
 1095 Atmos. Chem. Phys., 16, 2459-2475, 10.5194/acp-16-2459-2016, 2016.
- 1096 Thijssen, T. R., van Oss, R. F., and Lenschow, P.: Determination of Source Contributions to Ambient  
 1097 Volatile Organic Compound Concentrations in Berlin, Journal of the Air & Waste Management  
 1098 Association, 49, 1394-1404, 10.1080/10473289.1999.10463974, 1999.
- 1099 Urban, S.: Charakterisierung der Quellverteilung von Feinstaub und Stickoxiden in ländlichem und  
 1100 städtischem Gebiet, PhD, Mathematik und Naturwissenschaften, Bergischen Universität Wuppertal,  
 1101 Wuppertal, Germany, 2010.
- 1102 VDI: VDI Richtlinie 3871: Messen von Partikeln in der Außenluft - Elektrische Aerosolmonitore auf  
 1103 Basis der Diffusionsaufladung, in, edited by: Ingenieure, V. D., 2017.
- 1104 Villalobos, A. M., Barraza, F., Jorquera, H., and Schauer, J. J.: Chemical speciation and source  
 1105 apportionment of fine particulate matter in Santiago, Chile, 2013, Science of The Total Environment,  
 1106 512–513, 133-142, <http://dx.doi.org/10.1016/j.scitotenv.2015.01.006>, 2015.
- 1107 Volz-Thomas, A., Geiss, H., Hofzumahaus, A., and Becker, K. H.: Introduction to special section:  
 1108 Photochemistry experiment in BERLIOZ, Journal of Geophysical Research D: Atmospheres, 108, 1-1,  
 1109 2003.
- 1110 von Schneidmesser, E., Monks, P. S., and Plass-Duelmer, C.: Global comparison of VOC and CO  
 1111 observations in urban areas, Atmos. Environ., 44, 5053-5064,  
 1112 <https://doi.org/10.1016/j.atmosenv.2010.09.010>, 2010.
- 1113 von Schneidmesser, E., Monks, P. S., Gros, V., Gauduin, J., and Sanchez, O.: How important is  
 1114 biogenic isoprene in an urban environment? A study in London and Paris, Geophysical Research  
 1115 Letters, 38, 10.1029/2011GL048647, 2011.

1116 Wang, Y., Zhuang, G., Tang, A., Yuan, H., Sun, Y., Chen, S., and Zheng, A.: The ion chemistry and the  
1117 source of PM<sub>2.5</sub> aerosol in Beijing, *Atmos. Environ.*, 39, 3771-3784,  
1118 <http://dx.doi.org/10.1016/j.atmosenv.2005.03.013>, 2005.

1119 Watson, J. G., Cooper, J. A., and Huntzicker, J. J.: The effective variance weighting for least squares  
1120 calculations applied to the mass balance receptor model, *Atmospheric Environment* (1967), 18, 1347-  
1121 1355, [http://dx.doi.org/10.1016/0004-6981\(84\)90043-X](http://dx.doi.org/10.1016/0004-6981(84)90043-X), 1984.

1122 Weinhold, K.: personal communication, in, edited by: Gerwig, H., 2014.

1123 West, J. J., Smith, S. J., Silva, R. A., Naik, V., Zhang, Y., Adelman, Z., Fry, M. M., Anenberg, S., Horowitz,  
1124 L. W., and Lamarque, J.-F.: Co-benefits of mitigating global greenhouse gas emissions for future air  
1125 quality and human health, *Nature Clim. Change*, 3, 885-889, 10.1038/nclimate2009  
1126 [http://www.nature.com/nclimate/journal/v3/n10/abs/nclimate2009.html#supplementary-](http://www.nature.com/nclimate/journal/v3/n10/abs/nclimate2009.html#supplementary-information)  
1127 [information](http://www.nature.com/nclimate/journal/v3/n10/abs/nclimate2009.html#supplementary-information), 2013.

1128 Whalley, L. K., Stone, D., Bandy, B., Dunmore, R., Hamilton, J. F., Hopkins, J., Lee, J. D., Lewis, A. C.,  
1129 and Heard, D. E.: Atmospheric OH reactivity in central London: observations, model predictions and  
1130 estimates of in situ ozone production, *Atmos. Chem. Phys.*, 16, 2109-2122, 10.5194/acp-16-2109-  
1131 2016, 2016.

1132 WHO: WHO releases country estimates on air pollution exposure and health impact, in, World Health  
1133 Organization, Geneva, 2016.

1134 Wiedensohler, A., Wiesner, A., Weinhold, K., Birmili, W., Hermann, M., Merkel, M., Müller, T., Pfeifer,  
1135 S., Schmidt, A., Tuch, T., Velarde, F., Quincey, P., Seeger, S., and Nowak, A.: Mobility Particle Size  
1136 Spectrometers: Calibration Procedures and Measurement Uncertainties, *Aerosol Science and*  
1137 *Technology*, 10.1080/02786826.2017.1387229, 2017.

1138 Wiegner, M., Madonna, F., Biniotoglou, I., Forkel, R., Gasteiger, J., Geiß, A., Pappalardo, G., Schäfer,  
1139 K., and Thomas, W.: What is the benefit of ceilometers for aerosol remote sensing? An answer from  
1140 EARLINET, *Atmospheric Measurement Techniques*, 7, 1979-1997, 10.5194/amt-7-1979-2014, 2014.

1141 Wiegner, M., and Gasteiger, J.: Correction of water vapor absorption for aerosol remote sensing with  
1142 ceilometers, *Atmos. Meas. Tech.*, 8, 3971-3984, 10.5194/amt-8-3971-2015, 2015.

1143 Winkler, J., Blank, P., Glaser, K., Gomes, J. A. G., Habram, M., Jambert, C., Jaeschke, W., Konrad, S.,  
1144 Kurtenbach, R., Lenschow, P., Lörzer, J. C., Perros, P. E., Pesch, M., Prümke, H. J., Rappenglück, B.,  
1145 Schmitz, T., Slemr, F., Volz-Thomas, A., and Wickert, B.: Ground-Based and Airborne Measurements  
1146 of Nonmethane Hydrocarbons in BERLIOZ: Analysis and Selected Results, *Journal of Atmospheric*  
1147 *Chemistry*, 42, 465-492, 10.1023/a:1015709214016, 2002.

1148 WorldBank: The Cost of Air Pollution : Strengthening the Economic Case for Action, World Bank,  
1149 Washington, DC, 2016.

1150 Yang, H., Li, Q., and Yu, J. Z.: Comparison of two methods for the determination of water-soluble  
1151 organic carbon in atmospheric particles, *Atmos. Environ.*, 37, 865-870,  
1152 [http://dx.doi.org/10.1016/S1352-2310\(02\)00953-6](http://dx.doi.org/10.1016/S1352-2310(02)00953-6), 2003.

1153 Zhang, T., Claeys, M., Cachier, H., Dong, S., Wang, W., Maenhaut, W., and Liu, X.: Identification and  
1154 estimation of the biomass burning contribution to Beijing aerosol using levoglucosan as a molecular  
1155 marker, *Atmos. Environ.*, 42, 7013-7021, <http://dx.doi.org/10.1016/j.atmosenv.2008.04.050>, 2008.  
1156  
1157

## Figure Captions:

**Figure 1.** Location of the measurement station (MC042) and measurement van in Neukölln, Berlin. Maps show increasingly larger scale. The 'x's indicate sampling locations, with MC220 and MC143 indicating stations that record traffic counts. Map images from OpenStreetMap.

**Figure 2.** Time series of air pollutant concentrations, meteorological data, and benzene/toluene ratio measured as part of BLUME at the Neukölln station during the BAERLIN2014 campaign.

**Figure 3.** Time series of particulate matter mass, particle number, and lung depositable surface area concentrations measured at the Neukölln station during the BAERLIN2014 campaign. (a) BLUME PM10, (b) Grimm 1.108 PM10, (c) Grimm 1.108 PM2.5, (d) Grimm 1.108 PM1, (e) Grimm 1.108 PN, (f) Grimm 5.416 PN, (g) Grimm 5.403 PN, (h) NSAM LDSA. Units given in the y-axis label.

**Figure 4.** Mean diurnal cycles of the (top) particle number and (bottom) particle volume distributions at Neukölln. Legends show particle size bin range in nm.

**Figure 5.** Mean diurnal cycle of the particle number concentration by diameter.

**Figure 6.** Mean fractional contribution to mixing ratio (left column) and OH reactivity (right column) by compound class, based on a total mixing ratio or OH reactivity calculated from 57 compounds for 5 sampling locations throughout the city. Total number of canister samples for each location are Neukölln (18), Altlandsberg (10), Plänterwald (11), Tiergarten Tunnel (9), and the AVUS (2). The individual compounds included in each class are available in the SI.

**Figure 7.** Comparison between VOC measurements in this study and comparable previous work from June-August of 1996 (Thijssen et al., 1999). Compound classes are distinguished by color. Sampling locations by character.

**Figure 8.** Bulk composition analysis results from the PM10 filter samples, presented by filter groups, where GRA=Group A, GRB=Group B, etc. and B17, B19, B30 are individual filters. More information on the filter groups, including a some basic composition information and backtrajectory origin can be found in Table 3.

**Figure 9.** Molecular marker analysis results from the PM10 filter samples, presented by filter groups, where GRA=Group A, GRB=Group B, etc. and B17, B19, B30 are individual filters. More information on the filter groups, including a some basic composition information and backtrajectory origin can be found in Table 3.

**Figure 10.** Source contributions attributed to the OC fraction of the PM10 filter samples by filter groups, where GRA=Group A, GRB=Group B, etc. and B17, B19, B30 are individual filters. More information on the filter groups, including a some basic composition information and backtrajectory origin can be found in Table 3.



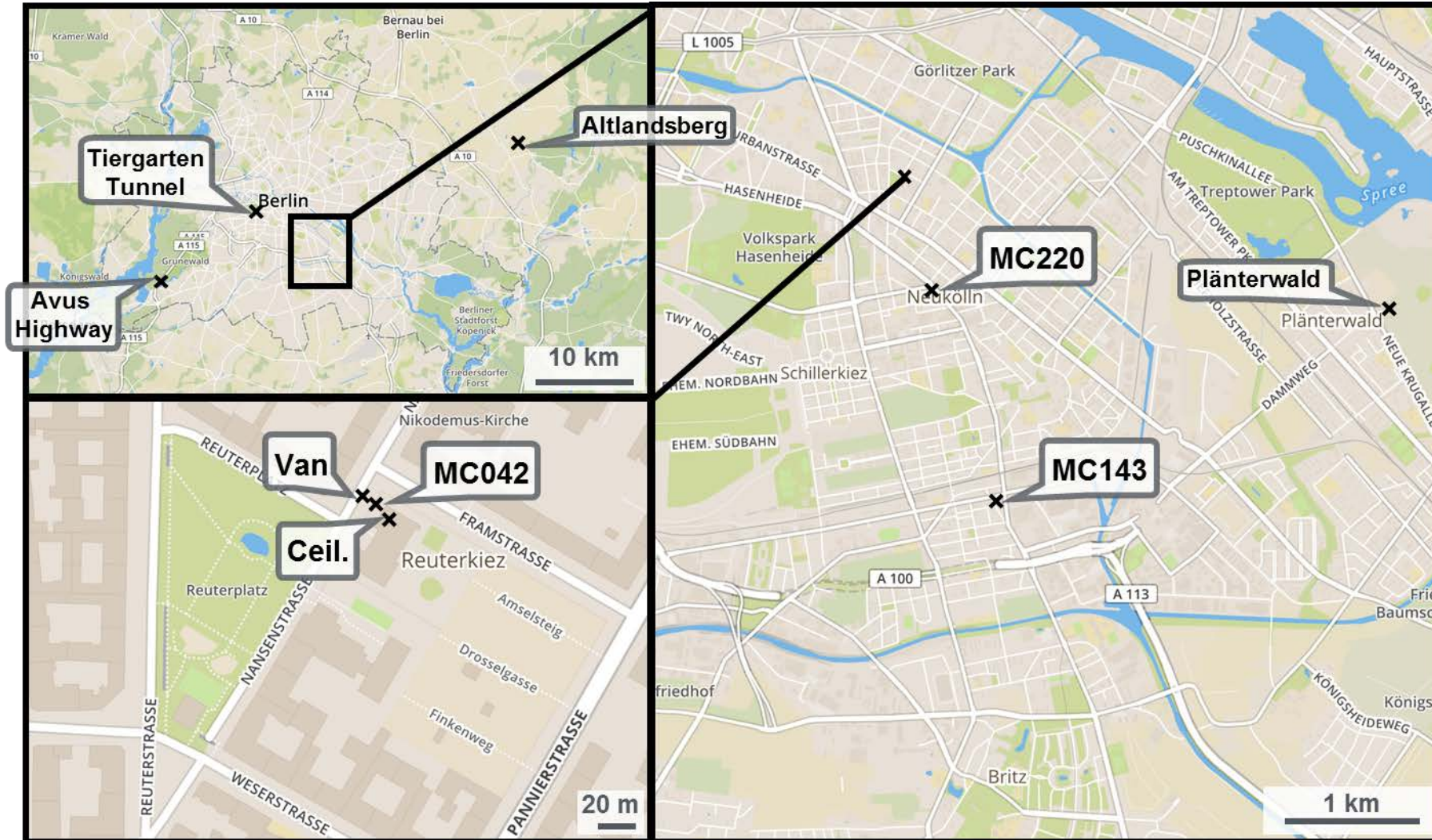


**Figure 1.** Location of the measurement station (MC042) and measurement van in Neukölln, Berlin. Maps show increasingly larger scale. The ‘x’ indicates sampling locations, with MC220 and MC143 indicating stations that record traffic counts. Map images from OpenStreetMap.

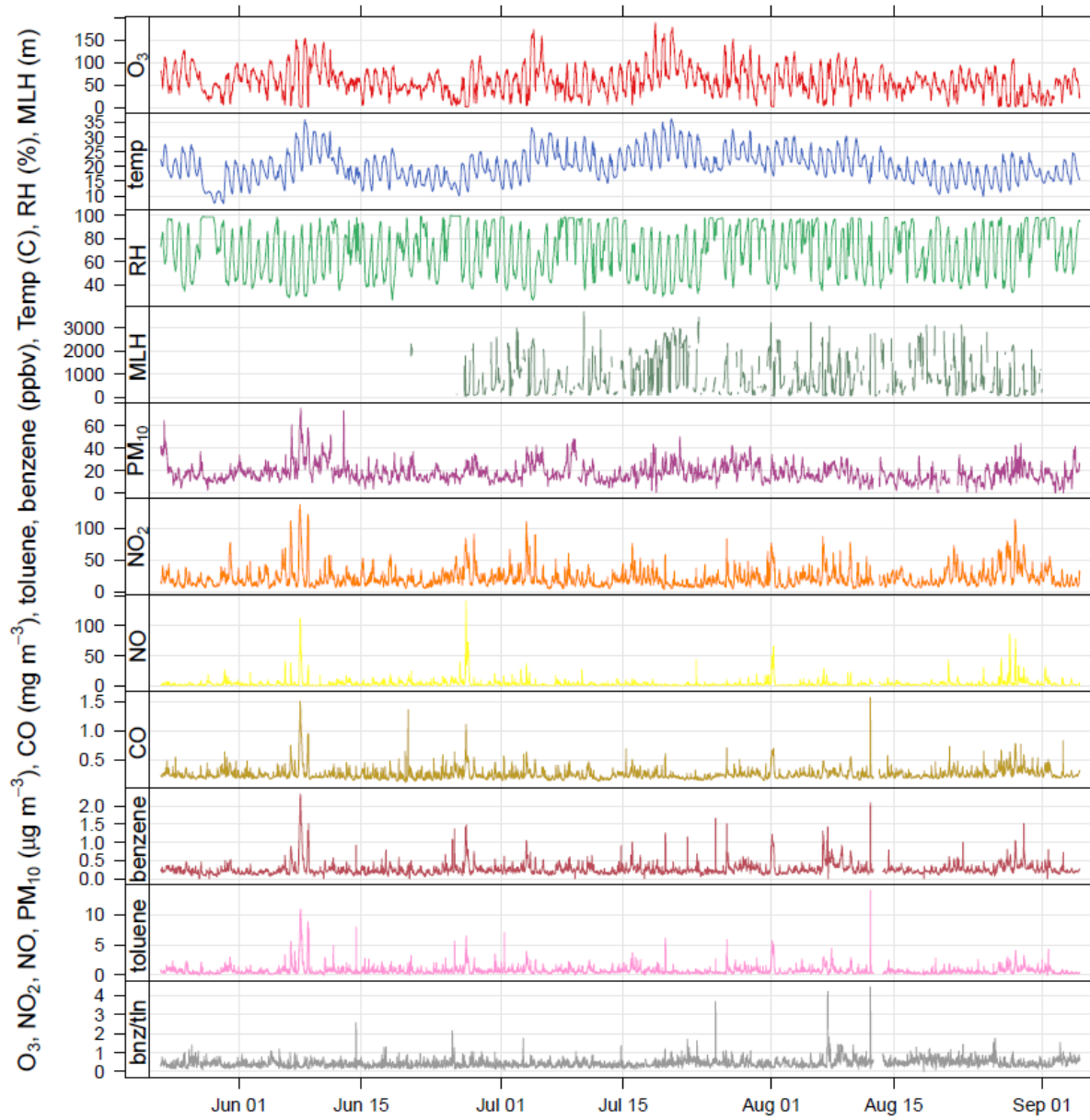


**Figure 2.** Time series of air pollutant concentrations, meteorological data, and benzene/toluene ratio measured as part of BLUME at the Neukölln station during the BAERLIN2014 campaign.

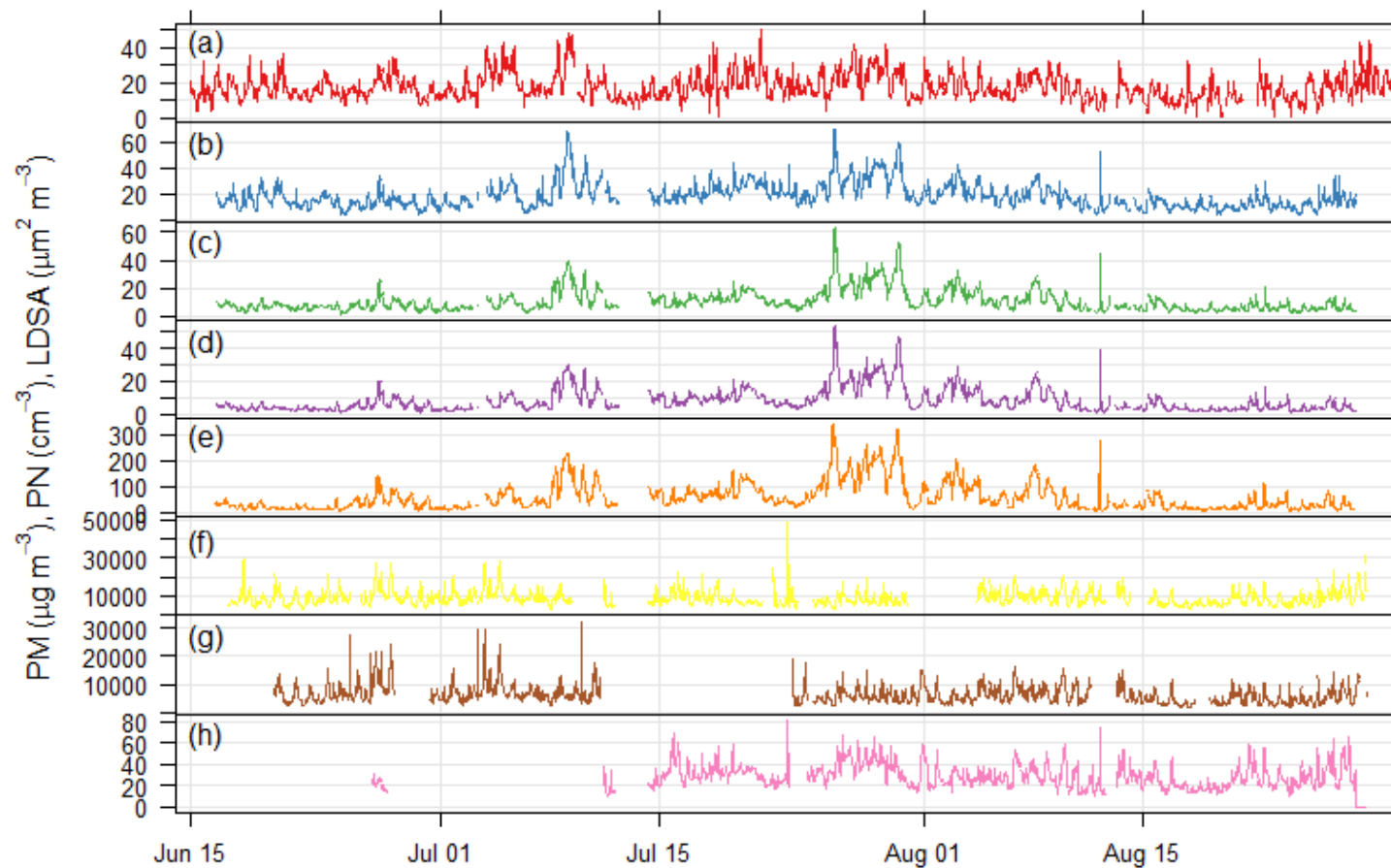


**Figure 3.** Time series of particulate matter mass, particle number, and lung depositable surface area concentrations measured at the Neukölln station during the BAERLIN2014 campaign. (a) BLUME PM10, (b) Grimm 1.108 PM10, (c) Grimm 1.108 PM2.5, (d) Grimm 1.108 PM1, (e) Grimm 1.108 PN, (f) Grimm 5.416 PN, (g) Grimm 5.403 PN, (h) NSAM LDSA. Units given in the y-axis label.



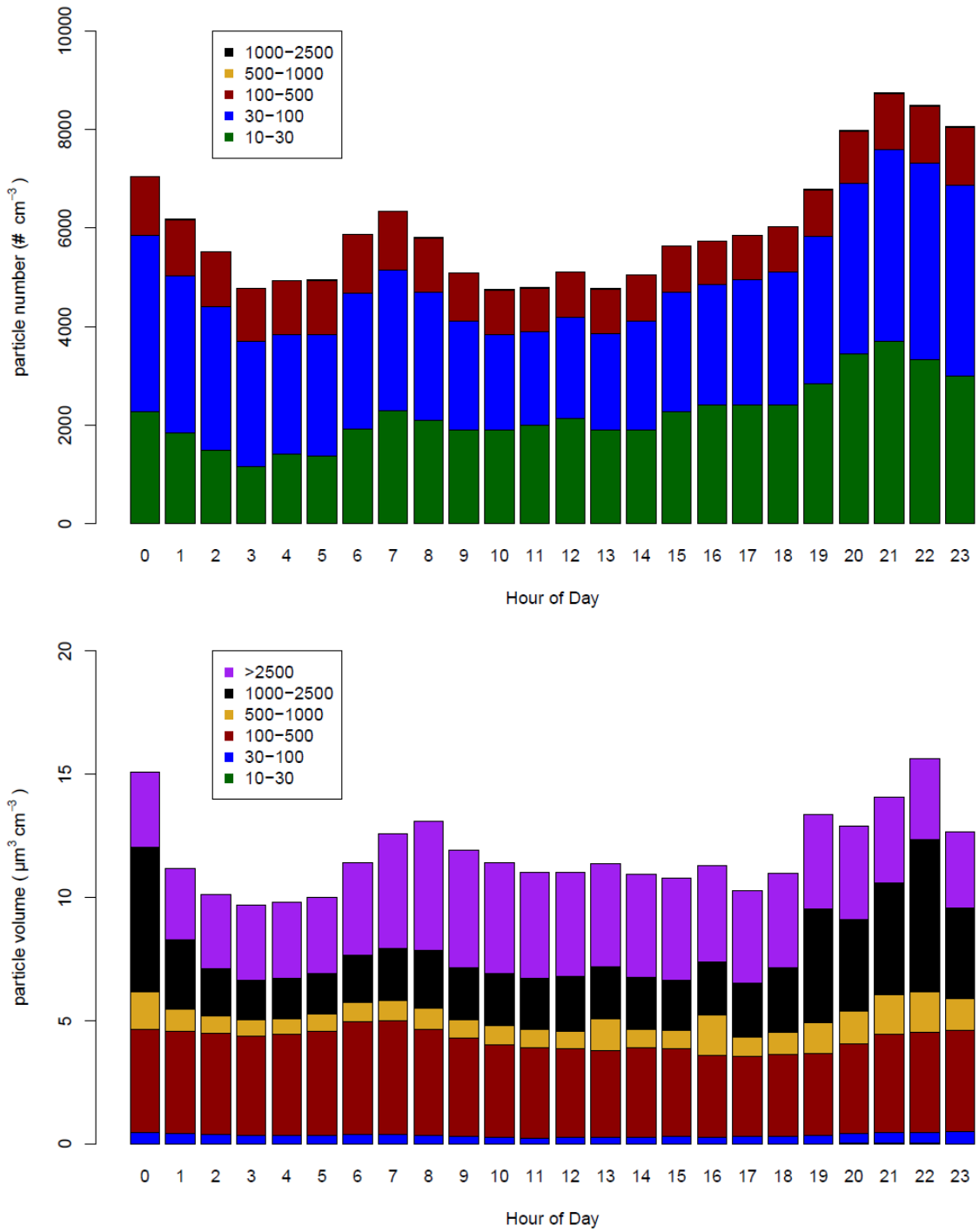


**Figure 4.** Mean diurnal cycles of the (top) particle number and (bottom) particle volume distributions at Neukölln. Legends show particle size bin range in nm.

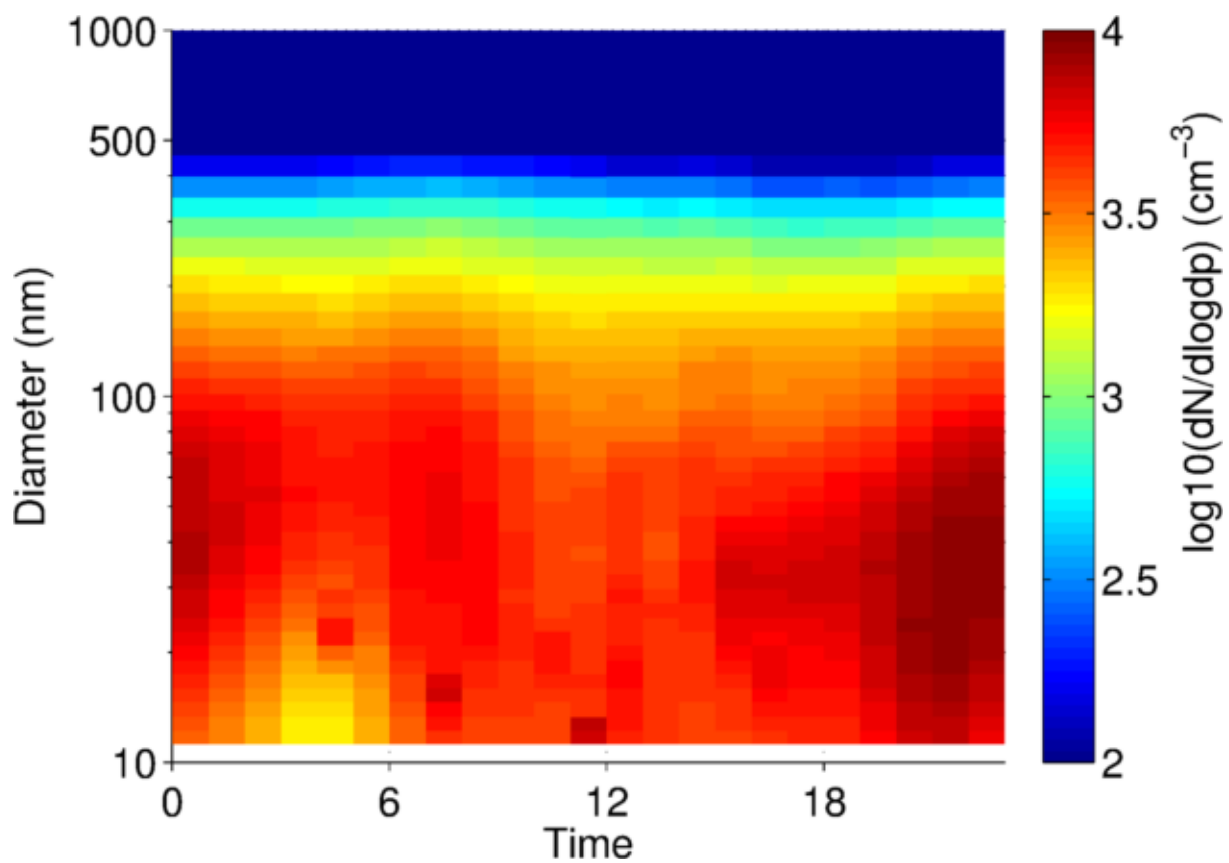


**Figure 5.** Mean diurnal cycle of the particle number concentration by diameter.

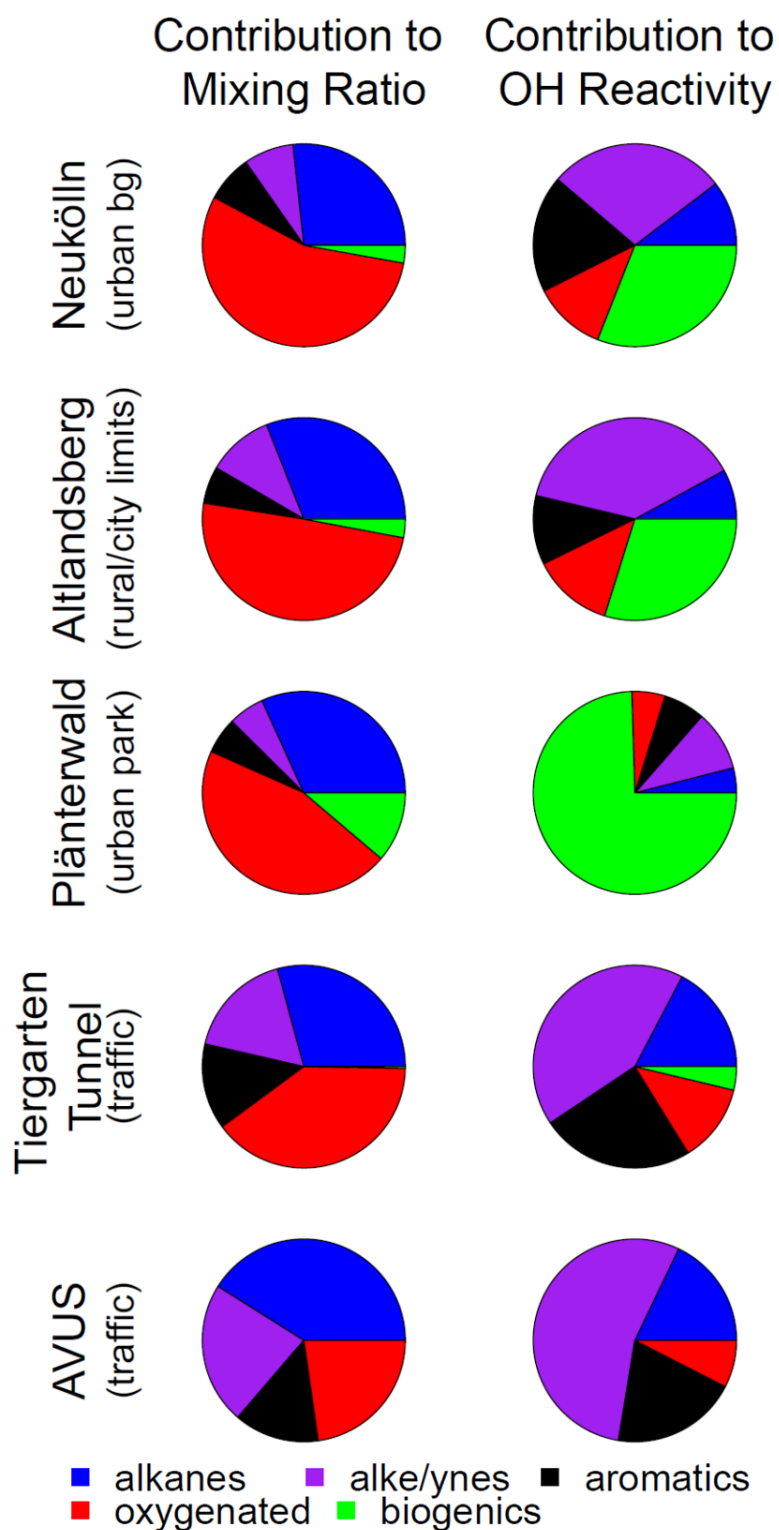


**Figure 6.** Mean fractional contribution to mixing ratio (left column) and OH reactivity (right column) by compound class, based on a total mixing ratio or OH reactivity calculated from 57 compounds for 5 sampling locations throughout the city. Total number of canister samples for each location are Neukölln (18), Altlandsberg (10), Plänterwald (11), Tiergarten Tunnel (9), and the AVUS (2). The individual compounds included in each class are available in the SI. For more information on the site classification, see Table 2.

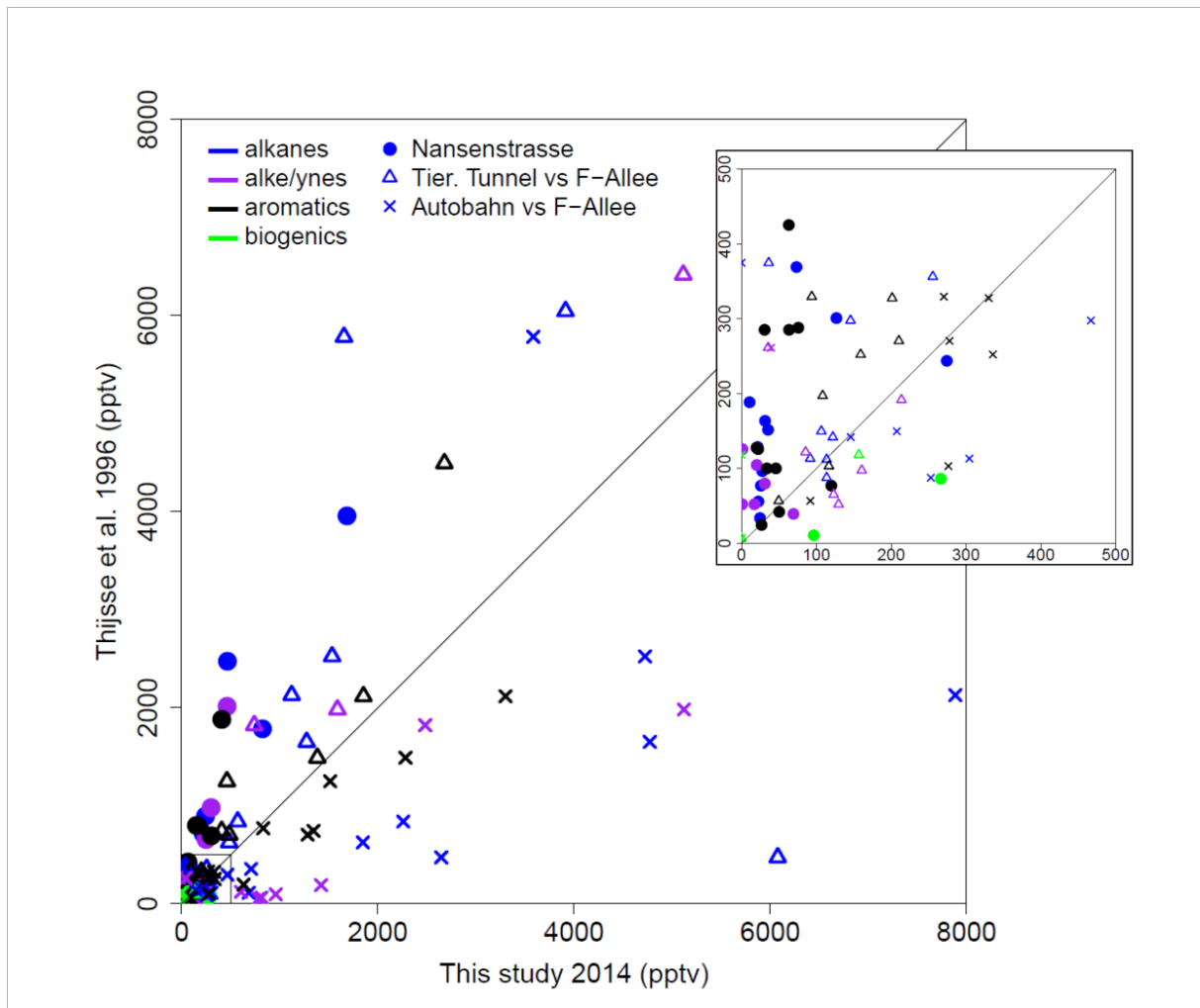


**Figure 7.** Comparison between VOC measurements in this study and comparable previous work from June-August of 1996 (Thijse et al., 1999). Compound classes are distinguished by color. Sampling locations by character.

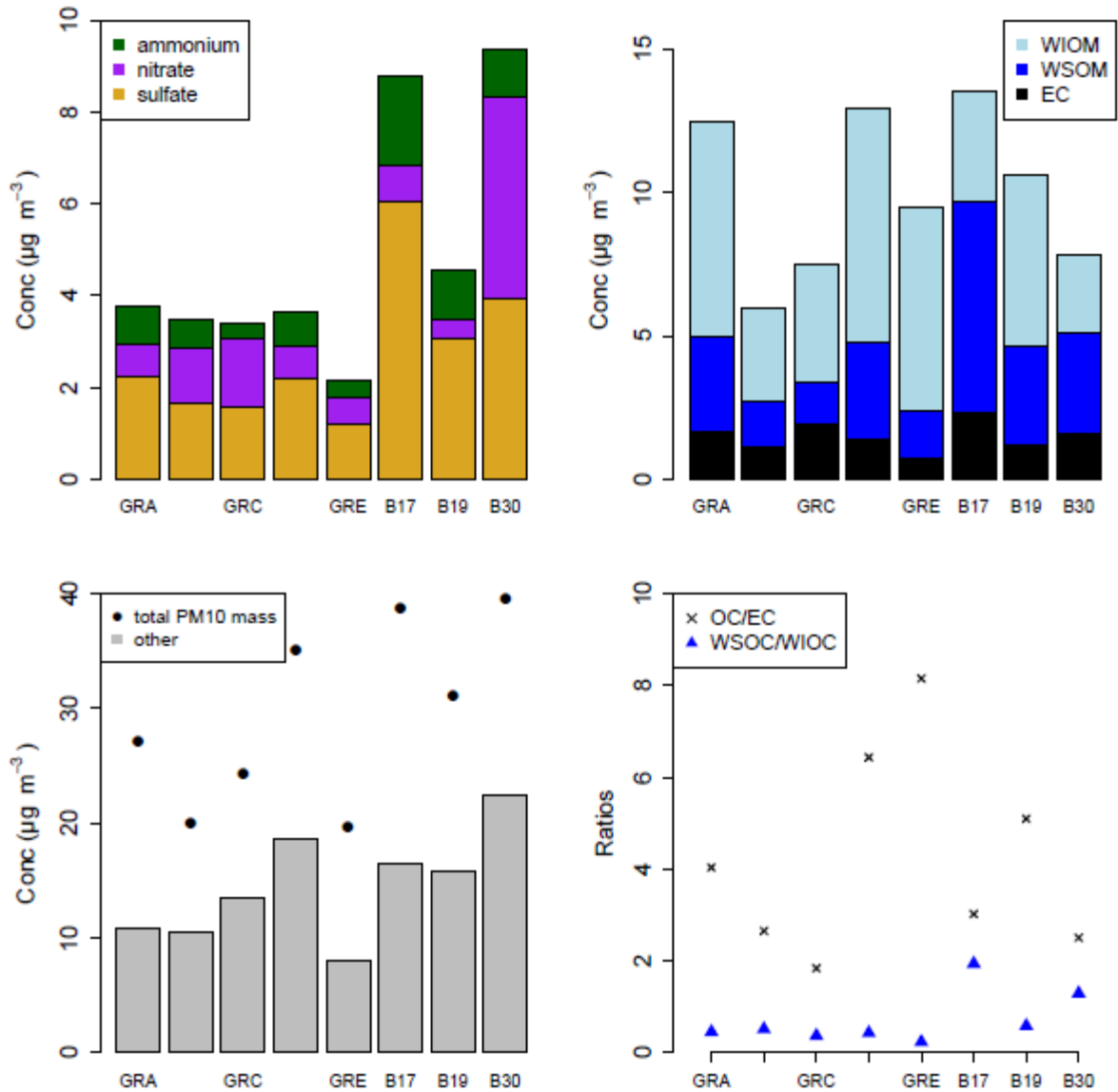


**Figure 8.** Bulk composition analysis results from the PM10 filter samples, presented by filter groups, where GRA=Group A, GRB=Group B, etc. and B17, B19, B30 are individual filters. More information on the filter groups, including a some basic composition information and backtrajectory origin can be found in Table 3.

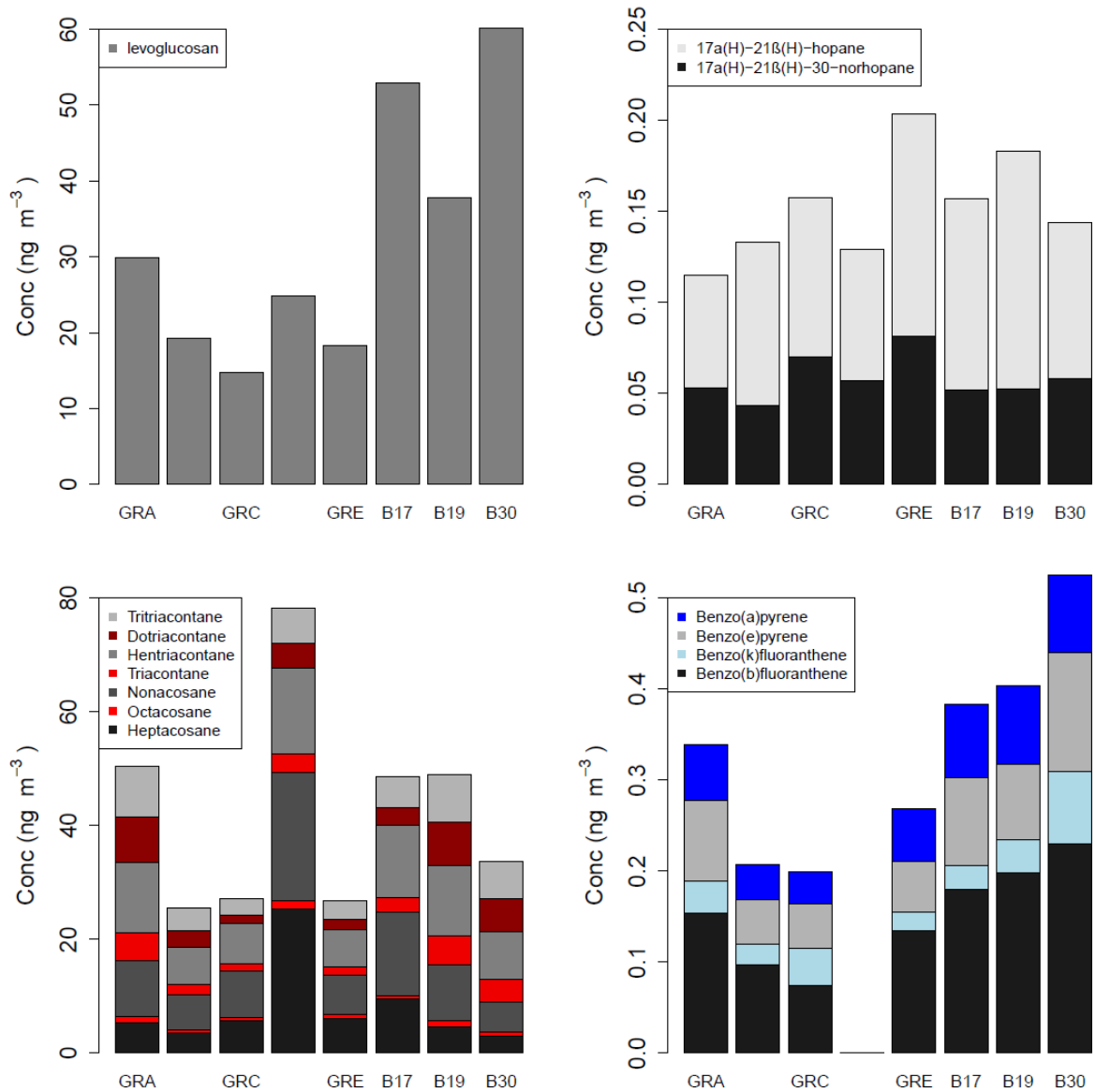


**Figure 9.** Molecular marker analysis results from the PM10 filter samples, presented by filter groups, where GRA=Group A, GRB=Group B, etc. and B17, B19, B30 are individual filters. More information on the filter groups, including a some basic composition information and backtrajectory origin can be found in Table 3.

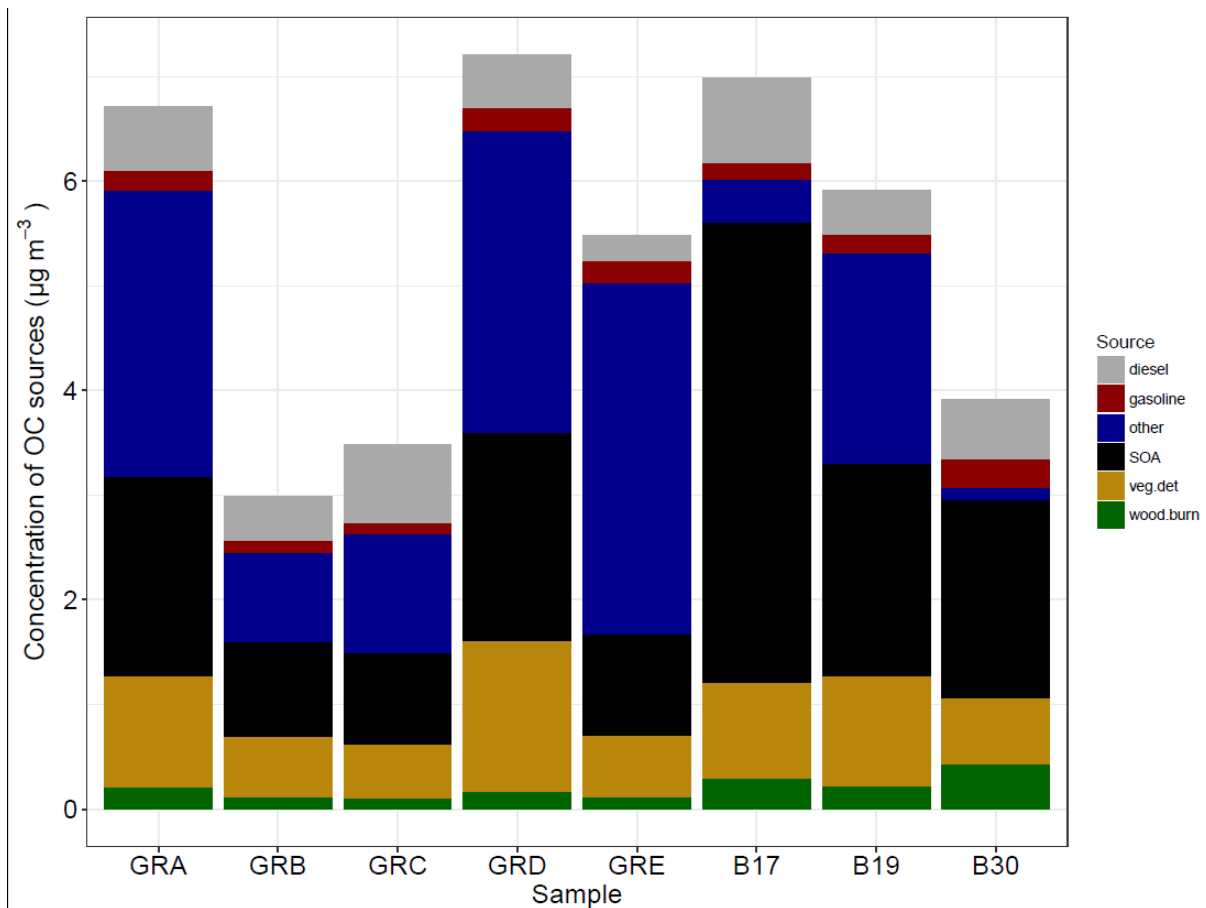


**Figure 10.** Source contributions attributed to the OC fraction of the PM10 filter samples by filter groups, where GRA=Group A, GRB=Group B, etc. and B17, B19, B30 are individual filters. More information on the filter groups, including a some basic composition information and backtrajectory origin can be found in Table 3.

**Table 1.** List of participating institutions and instruments deployed at the urban background site in Berlin (Nansenstrasse).

Institution	Instrument	Parameters	References
Berlin Senate	Leckel GmbH SEQ47/50 (x1)	PM <sub>10</sub>	DIN EN 16450:2015-10; Beuth, 2015
	Horiba APNA-370 Air Pollution Monitor	NO <sub>x</sub> , NO (measured directly); NO <sub>2</sub> (inferred)	DIN EN 14211:2005; Verbraucherschutz, 2010
	Horiba APOA-370 Air Pollution Monitor	O <sub>3</sub>	DIN EN 14625:2005; Verbraucherschutz, 2010
	Horiba APMA-370 Air Pollution Monitor	CO	DIN EN 14626:2005; Verbraucherschutz, 2010
	AMA Instruments GC5000 BTX	Benzene, toluene	DIN EN 14662:2005; Verbraucherschutz, 2010
KIT	Vaisala CL51 Ceilometer	Mixing layer height	Emeis et al., 2007; Münkler et al., 2007; Wiegner et al., 2014
UBA	GRIMM 1.108	Particle number and size distribution (350-22500 nm), 15 size bins	Görner et al. 2012
	GRIMM 5.403	Particle number and size distribution (10-1100 nm), 44 size bins	Heim et al., 2004
	GRIMM 5.416	Total particle number (4-3000 nm)	Helsper et al., 2008; Wiedensohler et al., 2017
	NSAM	Particle surface area (10-1000 nm)	Kaminski et al., 2013; VDI 2017
IASS	PTR-MS	NMVOCs (for a complete list of m/z see Table S1)	Bourtsoukidis et al. 2014
FZJ	Canister samples	NMVOCs (for a list of compounds, see Table 8 in Bonn et al., 2016, or for the 57 compounds included in this analysis the SI)	Urban 2010; Ehlers et al. 2016
	Filter sampling/analysis	PM <sub>10</sub> , mass, EC, OC	Kofahl 2012; Ehlers 2013
FMI-Helsinki	Cartridge samples	Biogenic NMVOCs	Mäki et al. 2017
UW-Madison	Filter analysis	WSOC, WIOC, ions, organic tracers	Yang et al., 2003; Wang et al., 2005; Miyazaki et al., 2011; Villalobos et al., 2015



**Table 2.** NMVOC canister sampling locations, site type, and average OH reactivity ( $\text{s}^{-1}$ )

	Location type	alkanes	alkenes	aromatics	oxygenated	biogenics	total
Neukölln†	Urban background station	0.27±0.10	0.75±0.40	0.49±0.29	0.29±0.08	0.82±0.44	2.6±0.68
Altlandsberg	Rural, agricultural area with a small town, partially forested	0.17±0.10	0.83±0.43	0.22±0.11	0.28±0.17	0.65±0.42	2.2±0.69
Plänterwald	approx. 1 km <sup>2</sup> urban park abutting the Spree river in eastern Berlin	0.20±0.06	0.47±0.14	0.33±0.12	0.25±0.04	3.7±0.90	4.9±1.0
Tiergarten Tunnel*	2.4 km tunnel, major 4-lane city thoroughfare in central Berlin	2.0±2.2	4.4±1.1	2.6±1.3	1.3±0.70	0.39±0.24	11±2.5
AVUS*	Highly trafficked motorway in western Berlin (traffic jam)	6.3±3.2	19±7.4	6.6±1.6	2.8±2.3	0.00±0.00	34±15

\* automated sampling while driving; all other samples taken from a stationary location.

† 20 minute sampling duration. All other samples had 10 minute sampling duration.

**Table 3.** Basic bulk composition results, ratios, and air mass origin from HYSPLIT. Units are  $\mu\text{g m}^{-3}$  unless otherwise noted. For OC and ED measurement uncertainty is included.

	Total PM10	Air mass origin (HYSPLIT)	Total OC ( $\pm$ unc)	Total EC ( $\pm$ unc)	Total Ions*	OC:EC ratio	WSOC of OC (%)	Ions:OC ratio**
Group A	27.1	Germany	$6.7 \pm 0.34$	$1.7 \pm 0.084$	5.1	4.0	31%	0.56
Group B	20.0	central Germany, northern France	$3.0 \pm 0.15$	$1.1 \pm 0.057$	5.3	2.7	34%	1.2
Group C	24.4	North Sea	$3.5 \pm 0.17$	$1.9 \pm 0.094$	5.7	1.8	27%	0.98
Group D	35.1	Baltic	$7.2 \pm 0.36$	$1.4 \pm 0.069$	5.0	6.4	30%	0.50
Group E	19.6	North Sea, Scandinavia, UK	$5.5 \pm 0.27$	$0.71 \pm 0.035$	3.2	8.1	19%	0.39
B17	38.8	Poland & east	$7.0 \pm 0.35$	$2.3 \pm 0.12$	11	3.0	66%	1.3
B19	31.0	Poland & north	$5.9 \pm 0.30$	$1.2 \pm 0.058$	6.0	5.1	37%	0.77
B30	39.5	Germany (northern France)	$3.9 \pm 0.20$	$1.6 \pm 0.078$	15	2.5	56%	2.4

\*Ions includes 7 species and is not limited to sulfate, nitrate, and ammonium.

\*\*Ratio of ions (sulfate, nitrate, ammonium) to OC

**Table 4.** Chemical mass balance source apportionment results. Units are  $\mu\text{g m}^{-3}$  unless otherwise noted. Uncertainty is measurement uncertainty, in the case of SOA propagated uncertainty.

	Total OC (unc)	% OC mass apportioned	measured WSOC (unc)	SOA* (unc)	veg. det. (std error)	wood burn. (std error)	diesel emissions (std error)	gasoline vehicles (std error)	R <sup>2</sup>	$\chi^2$
Group A	6.71± 0.34	30.8	2.06±0.10	1.91±0.11	1.07±0.13	0.21±0.04	0.61±0.06	0.19±0.02	0.77	12.39
Group B	2.99± 0.15	41.2	1.00±0.05	0.91±0.05	0.57±0.07	0.12±0.03	0.42±0.04	0.12±0.02	0.8	7.7
Group C	3.48± 0.17	42.4	0.94±0.05	0.87±0.05	0.52±0.06	0.10±0.02	0.74±0.07	0.11±0.02	0.85	5.38
Group D	7.21± 0.36	32.3	2.11±0.11	1.99±0.11	1.44±0.17	0.17±0.04	0.50±0.05	0.22±0.03	0.87	6.82
Group E	5.48± 0.27	21.2	1.05±0.05	0.97±0.06	0.59±0.07	0.12±0.03	0.24±0.03	0.21±0.02	0.77	9.78
B17	6.99± 0.35	31.1	4.61±0.23	4.40±0.24	0.91±0.10	0.30±0.07	0.81±0.08	0.15±0.03	0.8	7.89
B19	5.91± 0.30	31.7	2.19±0.11	2.03±0.12	1.05±0.12	0.22±0.05	0.42±0.04	0.18±0.03	0.73	9.83
B30	3.91± 0.20	48.6	2.21±0.11	1.90±0.13	0.63±0.08	0.44±0.09	0.57±0.06	0.28±0.04	0.76	10.17

\*The SOA contribution was not part of the CMB results, but rather calculated as: unapportioned WSOC (SOA) = measured WSOC – 0.71\*apportioned wood burning.